UNIVERSITA' DEGLI STUDI DI UDINE

**Corso di Dottorato di Ricerca in
Scienze e Tecnologie Cliniche
XXVII Ciclo**

TESI DI DOTTORATO DI RICERCA

**EVALUTATION OF FETAL CEREBRAL BLOOD FLOW
PERFUSION USING THREE DIMENSIONAL POWER
DOPPLER ULTRASOUND ANGIOGRAPHY IN FETUSES
AFFECTED BY INTRAUTERINE GROWTH RETARDATION**

Relatore:
Chiar.mo Prof. Diego Marchesoni

Dottorando:
Dott. Alberto Rossi

Anno Accademico 2013-2014

Table of Contents

Chapter 5
Evaluation of Fetal Cerebral Blood Flow using Power
Doppler Ultrasound Angiography in Fetuses affected by
Intrauterine Growth Restriction. A pilot study.

Chapter 1

Sonographic Bidimensional examination of the Fetal Brain
Guidelines for performing the "basic examination" and the "fetalneurosonogram"

1.1 General considerations

Gestational age

Ultrasound has been used for nearly 30 years as the main modality to help diagnose fetal CNS anomalies. The scope of guidelines is to review the technical aspects of an optimized approach to the evaluation of the fetal brain in surveys of fetal anatomy, that will be referred to in this chapter as a basic examination.

Detailed evaluation of the fetal CNS (fetal neurosonogram) is also possible but requires specific expertise and sophisticated ultrasound machines. This type of examination, at times complemented by three-dimensional ultrasound, is indicated in pregnancies at increased risk of CNS anomalies.

The appearance of the brain changes throughout gestation. To avoid diagnostic errors, it is important to be familiar with normal CNS appearances at different gestational ages. Most efforts to diagnose neural anomalies are focused around midgestation. Basic examinations are usually performed around 20 weeks'gestation.

The advantage of an early fetal neuroscan at 14–16 weeks is that the bones are thin and the brain may be evaluated from almost all angles.

Usually, a satisfying evaluation of the fetal CNS can always be obtained in the second and third trimesters of pregnancy. In late gestation, visualization of the intracranial structures is frequently hampered by the ossification of the calvarium.

Technical factors

Ultrasound transducers

High frequency ultrasound trandsucers increase spatial resolution but decrease the penetration of the sound beam. The choice of the optimal transducer and operating frequency is influenced by a number of factors including maternal habitus, fetal position and the approach used.

Most basic examinations are satisfactorily performed with 3–5-MHz transabdominal transducers.

Fetal neurosonography frequently requires transvaginal examinations that are usually conveniently performed with transducers between 5 and 10 MHz. (1,2) Three dimensional ultrasound may facilitate the examination of the fetal brain. (3, 4)

Imaging parameters

The examination is mostly performed with gray-scale bidimensional ultrasound. Harmonic imaging may enhance visualization of subtle anatomic details, particularly in patients who scan poorly. In neurosonographic studies, Color and power Doppler may be used, mainly to identify cerebral vessels. Proper adjustment of pulse repetition frequency (main cerebral arteries have velocities in the range of 20–40 cm/s during intrauterine life) and signal persistence enhances visualization of small vessels. (5)

1.2 Basic examination

Qualitative evaluation

Transabdominal sonography is the technique of choice to investigate the fetal CNS during late first, second and third trimesters of gestation in low risk pregnancies.

The examination should include the evaluation of the fetal head and spine.

Two axial planes allow visualization of the cerebral structures relevant to assess the anatomic integrity of the brain. (6)

These planes are commonly referred to as the transventricular plane and the transcerebellar plane.

A third plane, the so-called transthalamic plane, is frequently added, mostly for the purpose of biometry. (Figure 1)
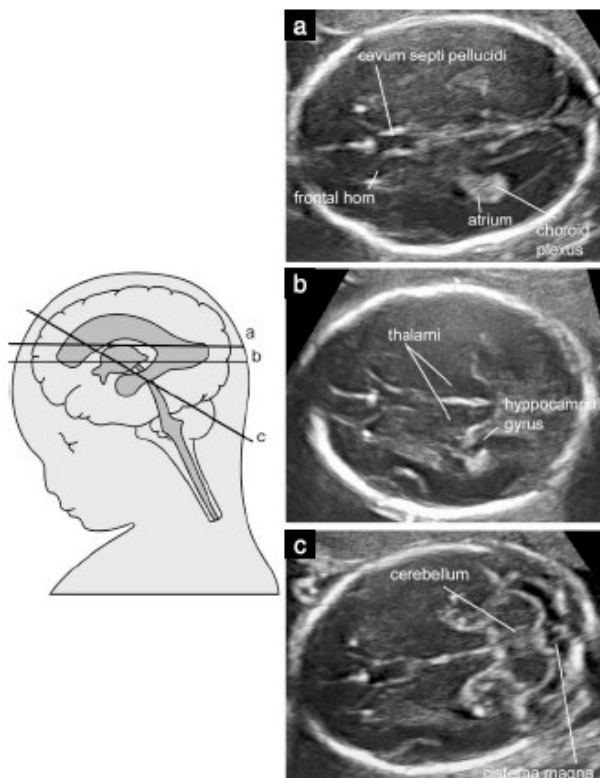

Figure 1 Axial views of the fetal head. (a) Transventricular plane; (b) transthalamic plane; (c) transcerebellar plane.

Structures that should be noted in the routine examination include the lateral ventricles, the cerebellum and cisterna magna, and cavum septi pellucidi. Head shape and brain texture should also be noted on these views. (Table 1)

Table 1 - Structures that are usually noted in a basic ultrasound examination of the fetal central nervous system
_____

Head shape
Lateral ventricles
Cavum septi pellucidi
Thalami
Cerebellum
Cisterna magna
Spine
_____

The transventricular plane

This plane demonstrates the anterior and posterior portion of the lateral ventricles. The anterior portion of the lateral ventricles (frontal or anterior horns) appears as two comma-shaped fluid filled structures. They have a well defined lateral wall and medially are separated by the cavum septi pellucidi (CSP).

The CSP is a fluid filled cavity between two thin membranes. In late gestation or the early neonatal period these membranes usually fuse to become the septum pellucidum. The CSP becomes visible around 16 weeks and undergoes obliteration near term gestation. With transabdominal ultrasound, it should always be visualized between 18 and 37 weeks, or with a biparietal diameter of 44–88 mm. (7)

Conversely, failure to demonstrate the CSP prior to 16 weeks or later than 37 weeks is a normal finding. The value of visualizing the CSP for identifying cerebral anomalies has been debated. However, this structure is easy to identify and is obviously altered with many cerebral lesions such as holoprosencephaly, agenesis of the corpus callosum, severe hydrocephaly and septo-optic dysplasia. (8)

From about 16 weeks the posterior portion of the lateral ventricles (also referred to as posterior horns) is in reality a complex formed by the atrium that continues posteriorly into the occipital horn.

The atrium is characterized by the presence of the glomus of the choroid plexus, which is brightly echogenic, while the occipital horn is fluid filled. Particularly in the second trimester of gestation both the medial and lateral walls of the ventricle are parallel to the midline and are therefore well depicted sonographically as bright lines.

Under normal conditions the glomus of the choroid plexus almost completely fills the cavity of the ventricle at the level of the atrium being closely apposed to both the medial or lateral walls, but in some normal cases a small amount of fluid may be present between the medial wall and the choroid plexus. (9, 10)

In the standard transventricular plane only the hemisphere on the far side of the transducer is usually clearly visualized, as the hemisphere close to the transducer is frequently obscured by artifacts. However, most severe cerebral lesions are bilateral or associated with a significant deviation or distortion of the midline echo, and it has been suggested that in basic examinations symmetry of the brain is assumed.

The transcerebellar plane

This plane is obtained at a slightly lower level than that of the transventricular plane and with a slight posterior tilting and includes visualization of the frontal horns of the lateral ventricles, CSP, thalami, cerebellum and cisterna magna. The cerebellum appears as a butterfly shake structure formed by the round cerebellar hemispheres joined in the middle by the slightly more echogenic cerebellar vermis. The cisterna magna or cisterna cerebello-medullaris is a fluid filled space posterior to the

cerebellum. It contains thin septations, that are normal structures and should not be confused with vascular structures or cystic abnormalities. In the second half of gestation the depth of the cisterna magna is stable and should be 2–10 mm. Early in gestation the cerebellar vermis has not completely covered the fourth ventricle, and this may give the false impression of a defect of the vermis. In later pregnancy such a finding may raise the suspicion of a cerebellar abnormality but prior to 20 weeks' gestation this is usually a normal finding. (11)

The Transthalamic plane

A third scanning plane, obtained at an intermediate level, is also frequently used in the sonographic assessment of the fetal head, and is commonly referred to as the transthalamic plane or biparietal diameter plane. The anatomic landmarks include, from anterior to posterior, the frontal horns of the lateral ventricles, the cavum septi pellucidi, the thalami and the hippocampal gyruses. (12)

Although this plane does not add significant anatomic information to that obtained from the transventricular and transcerebellar planes, it is used for biometry of the fetal head. It has been proposed that, particularly in late gestation, this section plane is easier to identify and allows more reproducible measurements than does the transventricular plane. (13)

1.3 Quantitative evaluation

Biometry is an essential part of the sonographic examination of the fetal head. In the second trimester and third trimester, a standard examination usually includes the measurement of the biparietal diameter, head circumference and internal diameter of

the atrium. Some also advocate measurement of the transverse cerebellar diameter and cisterna magna depth.

Biparietal diameter and head circumference are commonly used for assessing fetal age and growth and may also be useful to identify some cerebral anomalies. They may be measured either in the transventricular plane or in the transthalamic plane. Different techniques can be used for measuring the biparietal diameter. Most frequently the calipers are positioned outside the fetal calvarium (so called outside to outside measurement). (14)

However, some of the available charts have been produced using an outer to inner technique to avoid artifacts generated by the distal echo of the calvarium. The two approaches result in a difference of a few millimeters that may be clinically relevant in early gestation. It is important therefore to know the technique that was used while constructing the reference charts that one uses. If the ultrasound equipment has ellipse measurement capacity, then head circumference can be measured directly by placing the ellipse around the outside of the skull bone echoes. Alternatively, the head circumference (HC) can be calculated from biparietal diameter (BPD) and occipitiofrontal diameter (OFD) by using the equation HC = 1.62 Å~ (BPD + OFD). The ratio of the biparietal diameter over the occipitofrontal diameter is usually 75–85%. Moulding of the fetal head particularly in early gestation is however frequent, and most fetuses in breech presentation have some degree of dolicocephaly.

Measurement of the atrium is recommended because several studies suggest that this is the most effective approach for assessing the integrity of the ventricular system, and ventriculomegaly is a frequent marker of abnormal cerebral development. (15)

Measurement is obtained at the level of the glomus of the choroid plexus,

perpendicular to the ventricular cavity, positioning the calipers inside the echoes generated by the lateral walls. (Figure 2)

The measurement is stable in the second and early third trimesters, with a mean diameter of 6–8 mm and is considered normal when less than 10 mm. (16, 17, 18, 19, 20)

Most of the biometric studies on the size of the lateral ventricles have used ultrasound equipment that provided measurements in millimeters. (21)

As, with modern equipment, measurements are given in tenths of millimeters, it is uncertain which is the most reasonable cut-off value. We believe that particularly at midgestation a value of 10.0 mm or greater should be considered suspicious. (22)

The transverse cerebellar diameter increases by about one millimeter per week of pregnancy between 14 and 21 menstrual weeks. This measurement, along with the head circumference and the biparietal diameter is helpful to assess fetal growth.

The depth of the cisterna magna measured between the cerebellar vermis and the internal side of the occipital bone is usually 2–10 mm. (23) With dolicocephaly, measurements slightly larger than 10 mm may be encountered.
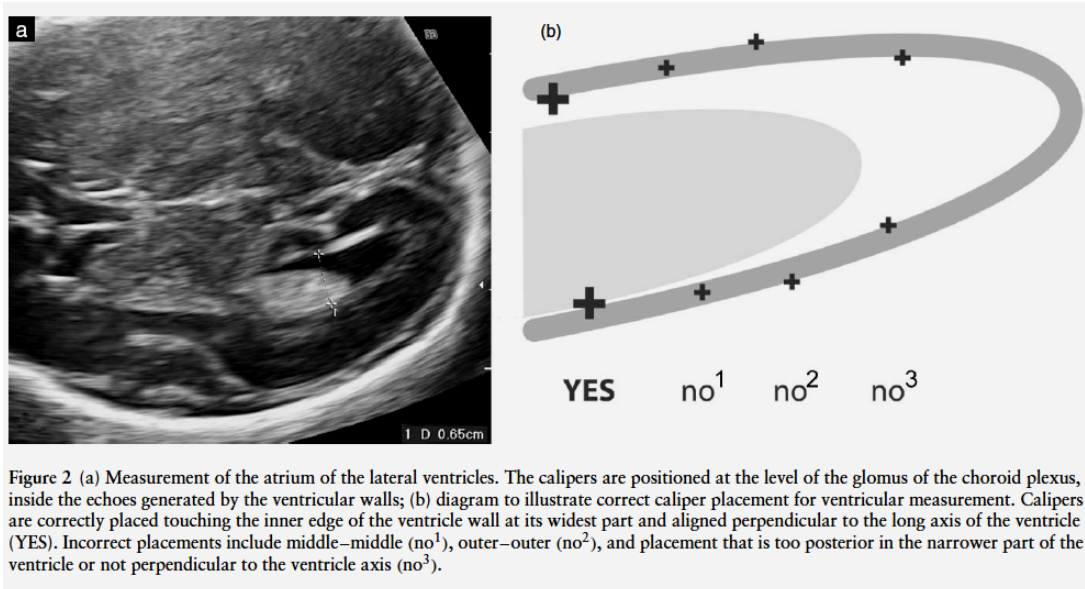
Figure 2 (a) Measurement of the atrium of the lateral ventricles. The calipers are positioned at the level of the glomus of the choroid plexus, inside the echoes generated by the ventricular walls; (b) diagram to illustrate correct caliper placement for ventricular measurement. Calipers are correctly placed touching the inner edge of the ventricle wall at its widest part and aligned perpendicular to the long axis of the ventricle (YES). Incorrect placements include middle–middle (no[1]), outer–outer (no[2]), and placement that is too posterior in the narrower part of the ventricle or not perpendicular to the ventricle axis (no[3]).

1.4 Fetal Neurosonogram

It is commonly accepted that dedicated fetal neurosonography has a much greater diagnostic potential than that of the standard transabdominal examination, and is particularly helpful in the evaluation of complex malformations.

However, this examination requires a grade of expertise that is not available in many settings and the method is not yet universally used.

Dedicated fetal neurosonography is useful in patients with an increased risk of CNS anomalies, including cases in which the basic examination identifies suspicious findings.

The basis of the neurosonographic examination of the fetal brain is the multiplanar approach, that is obtained by aligning the transducer with the sutures and fontanelles of the fetal head. (1, 24)

When the fetus is in vertex presentation, a transabdominal/transvaginal approach can be used. In fetuses in breech presentation, a transfundal approach is used, positioning the probe parallel instead of perpendicular to the abdomen. Vaginal probes have the

advantage of operating at a higher frequency than do abdominal probes and therefore allow a greater definition of anatomical details. For this reason, in some breech presenting fetuses an external cephalic version may be considered in order to use the transvaginal approach.

Fetal brain

Whether the exam is performed transvaginally or transabdominally, proper alignment of the probe along the correct section planes usually requires gentle manipulation of the fetus. A variety of scanning planes can be used, also depending upon the position of the fetus. (1)

A systematic evaluation of the brain usually includes the visualization of four coronal and three sagittal planes.

In the following, a description of the different structures that can be imaged in the late second and third trimesters is reported. Apart from the anatomic structures, fetal neurosonography should also include evaluation of the convolutions of the fetal brain that change throughout gestation. (24, 25, 26, 27, 28)

Coronal planes (Figure 3)

The transfrontal plane or Frontal-2 plane. The visualization of this plane is obtained through the anterior fontanelle and depicts the midline interhemispheric fissure and the anterior horns of the lateral ventricles on each side. The plane is rostral to the genu of the corpus callosum and this explains the presence of an uninterrupted interhemispheric fissure. Other structures observed are the sphenoidal bone and the ocular orbits. (22)

The transcaudate plane or Mid-coronal-1 plane

At the level of the caudate nuclei, the genu or anterior portion of the corpus callosum interrupts the continuity of the interhemispheric fissure. Due to the thickness of the genu in coronal planes it is observed as a more echogenic structure than the body of the corpus callosum.

The cavum septi pellucidi is depicted as an anechogenic triangular structure under the corpus callosum. The lateral ventricles are found at each side surrounded by the brain cortex. In a more lateral position the Sylvian fissures are clearly identified. (22)
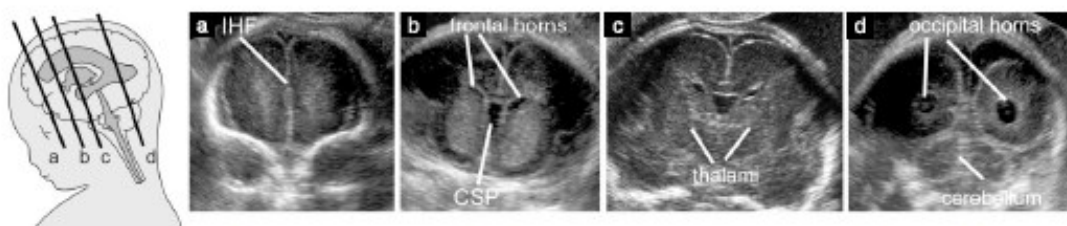
Figure 3 Coronal views of the fetal head. (a) Transfrontal plane; (b) transcaudate plane; (c) transthalamic plane; (d) transcerebellar plane. CSP, *cavum septi pellucidi*; IHF, interhemispheric fissure.
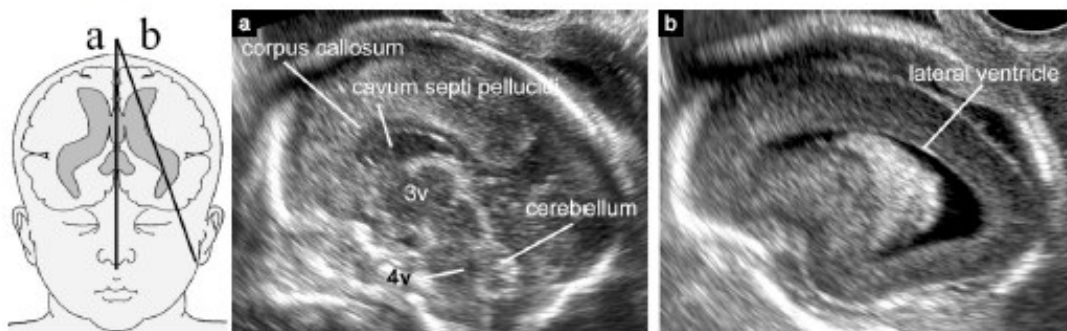
Figure 4 Sagittal planes of the fetal head. (a) Midsagittal plane; (b) parasagittal plane. 3v, third ventricle; 4v, fourth ventricle.

The transthalamic plane or Mid-coronal-2 plane

Both thalami are found in close apposition but in some cases the third ventricle may be observed in the midline with the interventricular foramina and the atrium of the lateral ventricles with the choroid plexus slightly cranial on each side (Mid-coronal-3

plane). Close to the cranial base and in the midline the basal cistern contains the vessels of the circle of Willis and the optic chiasma. (22)

The transcerebellar plane or Occipital-1 and 2 plane.

This plane is obtained through the posterior fontanels and enables visualization of the occipital horns of the lateral ventricles and the interhemispheric fissure. Both cerebellar hemispheres and the vermis are also seen in this plane. (22)

Sagittal planes (Figure 4)

Three sagittal planes are usually studied: the midsagittal; and the parasagittal of each side of the brain.

The *midsagittal or median plane* shows the corpus callosum with all its components; the cavum septi pellucidi, and in some cases also the cavum vergae and cavum veli interpositi, the brain stem, pons, vermis and posterior fossa. Using color Doppler the anterior cerebral artery, pericallosal artery with their branches and the vein of Galen may be seen.

The *parasagittal or Oblique plane* depicts the entire lateral ventricle, the choroid plexus, the periventricular tissue and the cortex. (22)

1.5 Effectiveness of Ultrasound Examination of the Fetal Neural Axis

In a low risk pregnancy around midgestation, if the transventricular plane and the

transcerebellar plane are satisfactorily obtained, the head measurements (head circumference in particular) are within normal limits for gestational age, the atrial width is less than 10.0 mm and the cisterna magna width is between 2–10 mm, many cerebral malformations are excluded, the risk of a CNS anomaly is exceedingly low and further examinations are not indicated. (22)

It is beyond the scope of these guidelines to review the available literature on the sensitivity of antenatal ultrasound in the prediction of neural anomalies. Some studies of low risk patients undergoing basic examinations have reported sensitivities in excess of 80%. (29, 30)

However, these results probably greatly overestimate the diagnostic potential of the technique. These surveys had invariably very short follow-up and almost only included open neural tube defects, whose recognition was probably facilitated by systematic screening with maternal serum alphafetoprotein.

Diagnostic limitations of prenatal ultrasound are well documented and occur for a number of reasons. Some even severe anomalies may be associated with only subtle findings in early gestation.

The brain continues to develop in the second half of gestation and into the neonatal period thus limiting the detection of anomalies of neuronal proliferation (such as microcephaly, tumors and cortical malformations). (31)

Also, some cerebral lesions are not due to faulty embryological development but represent the consequence of acquired prenatal or perinatal insults. Even in expert hands some types of anomalies may be difficult or impossible to diagnose in utero, in a proportion that is yet impossible to determine with precision. (22)

Chapter 2

Intracranial Fetal Vascularization

Anatomy of Cerebral Blood Arteries

2.1 Extracranial Origins

The brain is supplied by four arteries: two internal carotids (ictd) and two vertebrals (vert).

The contributions of blood flow to the brain by these arteries is almost three fourths of the total for the carotids and one fourth for the vertebrals. All these vessels originate from branches stemming out of the aortic arch (ao). (32)

Phylogenetically, six branchial arches are identified of which in mammals the fourth gives origin to the aortic arch on the left and the subclavia artery (sbcl) on the right.

The third branchial arch and the remnants of the primitive dorsal aorta originate the internal carotid, while the remnants of the primitive ventral aorta turn into the external carotid (ectd).

A brachiocephalic trunk (bcph) originates from the convexity of the aorta and gives origin to the right subclavian and right common carotid artery (cctd).

On the left side, the common carotid and subclavian arteries originate separately from the aorta to the left of the brachiocephalic trunk origin.

The vertebral arteries originate from the subclavians and run dorsally and medially to

reach the transverse foramen of the sixth cervical vertebra (C6). They continue rostrally within the transverse canal, formed by the superposition of the transverse foraminae of the cervical vertebrae. (33)

The forebrain (telencephalon and diencephalon) receives its arterial supply from the internal carotids, which divide intracranially into the anterior (acer), middle (mcer) cerebral arteries (Figure 1) and the anterior choroidal artery.

The hindbrain (metencephalon and myelencephalon) as well as the mesencephalon receive their arterial supply from the vertebral arteries (Figure 2), which join to form the basilar artery (Figure 2 – Figure 3).

This vessel inturn divides into the two posterior cerebral arteries (Figure 2 – Figure 3).

The carotid and the vertebrobasilar system are connected by a pair of posterior communicating arteries (pcoma) (Figure 3). (34)
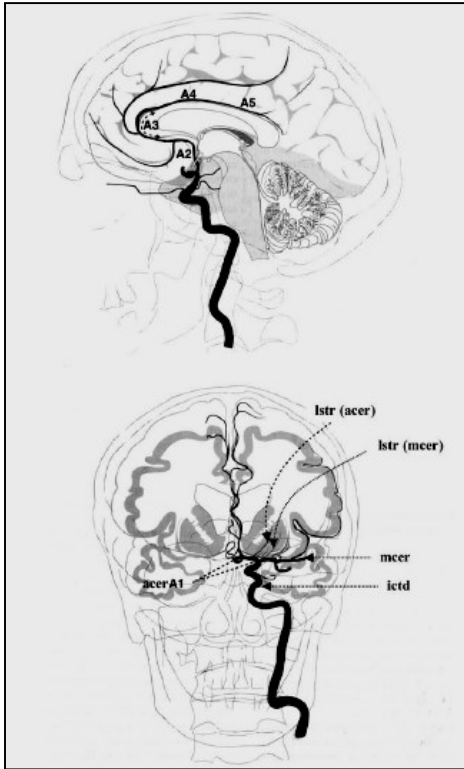
Figure 1 - Segmental anatomy of the anterior cerebral artery in sagittal (top) and coronal (bottom) projections.
The segments of this artery are defined thus: A1 from the internal carotid artery bifurcation to the anterior communicating, A2 to the junction of genu and rostrum of the corpus callosum, A3 around the genu, A4 to the plane of the coronal suture and A5 from the coronal suture to the terminal branches. 1str, lenticulo striate arteries from anterior cerebral (acer) and middle cerebral (mcer); ictd, internal carotid artery.
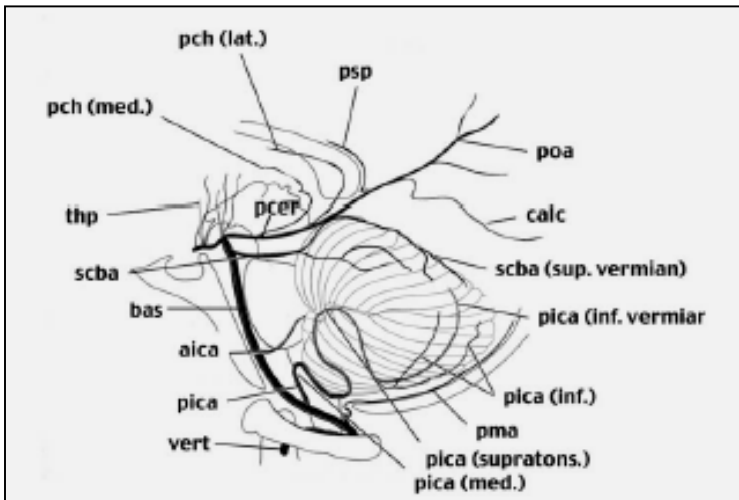
Figure 2 - Projection on the sagittal plane of the posterior arterial circulation.
Vert, vertebral artery; pica, posterior inferior cerebellar; its medullary (med), and supratonsilar (supratons) segments, and its inferior hemispheric (inf) and inferior vermian (inf. Vermian) branches; bas, basilar; aica, anterior inferior cerebellar; scba, superior cerebellar with its superior vermian (sup. Vermian) branch; pcer, posterior cerebral; thp, thalamo perforating; calc, calcarine; poa, parieto occipital; psp, perisplenial; pch (lat), lateral posterior choroidal; pch (med), medial posterior choroidal.

19
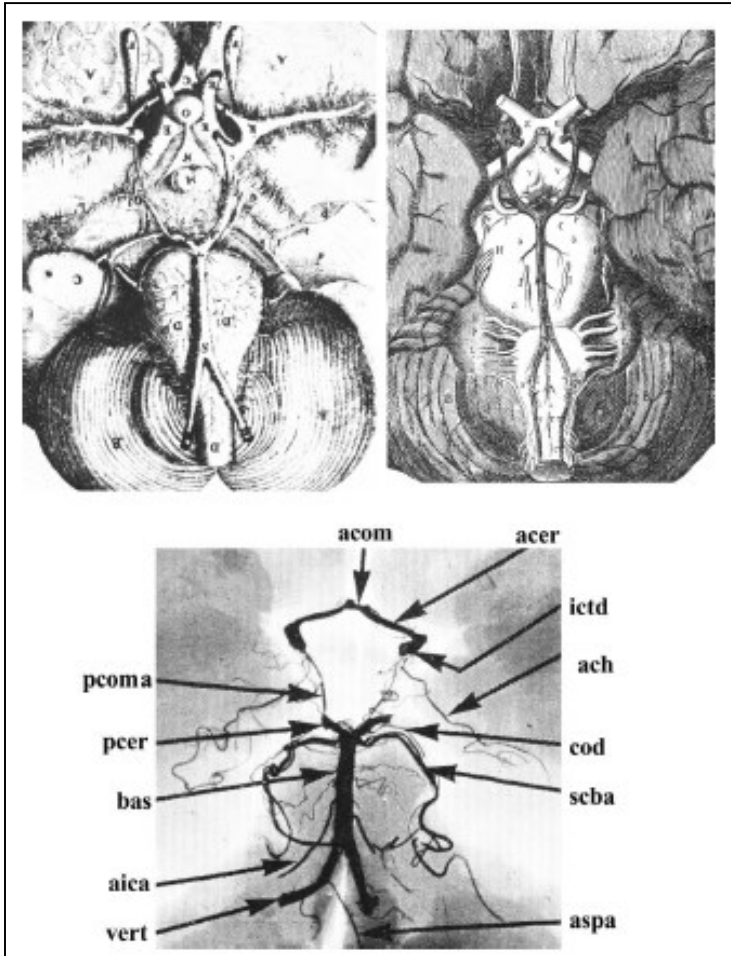
Figure 3 - X-ray image obtained after injection of radioopaque material postmortem. Acom, anterior communicating; acer, anterior cerebral; ictd, internal carotid; ach, anterior choroidal; cod, choroidal-diencephalic; scba, superior cerebellar; aspa, anterior spinal; vert, vertebral; aica, anterior inferior cerebellar; bas, basilar; pcer, posterior cerebral; pcoma, posterior communicating.

2.2 The Carotid System

The common carotid bifurcates into an external and an internal carotid at or slightly below the level of the hyoid bone, on the projection of the C3-C4 or C4-C5 vertebrae. The internal carotid then courses in a cephalad direction, medial to the internal jugular vein with the vagus nerve interposed between the two vessels.

The internal carotid artery lies first posterolaterally and then medially to the external carotid artery.

The internal carotid artery lies inside a major sinus (cavernous), which drains blood

from the orbit and nasal cavities. After the internal carotid artery exits the cavernous sinus, it gives off the ophthalmic artery (oph), which provides the main arterial supply to the eye and the orbital contents. In the early stages of human development (35 day,12–14 mm embryo), the internal carotid artery divides intracranially into four vessels: anterior, middle, and posterior cerebral (pcer), and anterior choroidal (ach) arteries. (Figure 4) (35)

The posterior cerebral arteries anastomose caudally with the two terminal branches of the basilar artery, which supply the ventral mesencephalon and continue beyond that point to supply the dorsal mesencephalon and caudal portion of the diencephalon. As the telencephalon develops, the posterior cerebral artery also supplies its caudal portion. Up until birth, the entire territory of the posterior cerebral artery appears to be supplied from the internal carotid artery.

Anterior cerebral artery courses rostromedially, dorsal to the optic nerve, to reach the interhemispheric fissure. At the midline, it anastomoses with its contralateral homonymous vessel through the anterior communicating artery. (acom) (Figure 3)

Along its precommunicating segment (A1), the anterior cerebral artery supplies perforator branches to the septal nuclei, the anterior portion of the hypothalamus, including the supraoptic nuclei, and the anterior portion of the striatum. (lenticulostriate arteries, lstr) (Figure 1)
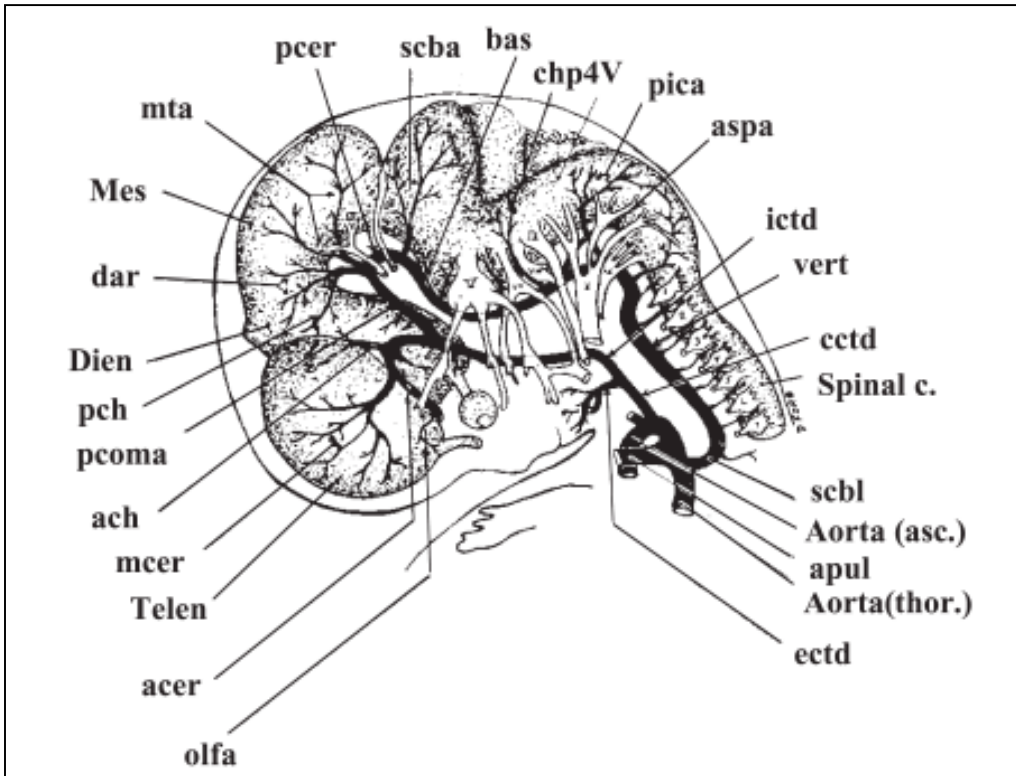
Figure 4 - Continuity of the great anastomotic arch between common carotid and subclavian arteries established in the embryo (shown in this figure as representation at 35 days of age). Structures abbreviations: Telen, telencephalon; Mes, mesencephalon; chp4v, choroid plexus of fourth ventricle; Spinal c., cervical spinal cord. Arteries abbreviations: olfa, primitive olfactory; acer, anterior cerebral; mcer, middle cerebral; arch, anterior choroidal; pcoma, posterior communicating; pch, posterior choroidal; dar, diencephalic; mta, mesencephalic tectum arteries; pcer, posterior cerebral; scba, superior cerebellar; bas, basilar; pica, posterior inferior cerebellar; aspa, anterior spinal; ictd, internal carotid; cctd, common carotid; scbls, subclavian; Aorta (asc.) , ascending aorta; apul, pulmonary; aorta (thor.), thoracic aorta; ectd, external carotid.
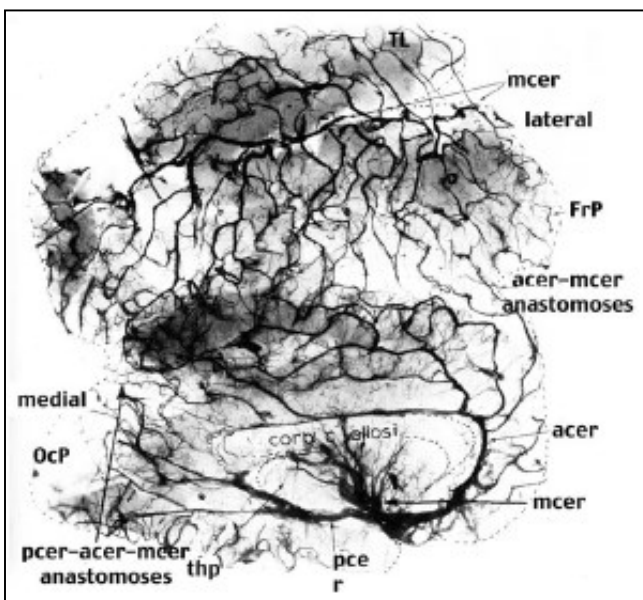

Figure 5 - Postmortem angiogram in which the entire cerebral cortex has been flattened to show the multiple anastomoses between the territories of the anterior (acer), middle (mcer) and posterior (pcer) cerebral arteries. The thalamo - perforating branches (thp) are also shown. The corpus callosum is outlined for reference, OcP, occipital pole; FrP, frontal pole; TL, temporal lobe.

The anterior cerebral artery continues rostrodorsally, curves around the genu of the corpus callosum as the pericallosal artery supplies the medial aspect of the frontal lobe (Figure 1) through the internal frontal branches (anterior, middle, and posterior) as well as the corpus callosum, its adjacent cortex, septum pellucidum, anterior pillars of the fornix, and the anterior commissure. Its largest branch, the callosomarginal artery, courses laterally into the cingulate sulcus. The terminal portion of the anterior cerebral artery branches anastomose with the cortical and perisplenial branches of the posterior cerebral artery. The medial aspects of both hemispheres could be irrigated from a single anterior cerebral artery, when a pericallosal artery provides branches to the contralateral side, or even more completely when an azygos (unpaired) anterior cerebral artery is present. (36)

The middle cerebral artery is considered the continuation of the internal carotid. It is a vessel of paramount functional significance since in its territory are found the cortical representations of motor, somatosensory, language, and higher cognitive functions. It also provides irrigation to most of the striatum and long ascending and descending tracts. This artery originates from the internal carotid artery just lateral to the optic chiasm, and then it proceeds laterally, ventral to the olfactory trigone to enter the Sylvian fissure.

The middle cerebral artery is considered the continuation of the internal carotid, it originates from this vessel just lateral to the optic chiasm, and then it proceeds laterally, ventral to the olfactory trigone to enter the Sylvian fissure. In its territory are found the cortical representations of motor, somatosensory, language, and higher cognitive functions. It also provides irrigation to most of the striatum and long ascending and descending tracts.

Along the middle cerebral artery proximal trajectory, a variable number of perforators arise from its dorsal aspect and penetrate the base of the brain through the anterior perforated substance. (Figure 1) The middle cerebral artery divides into its cortical branches generally at the level of the limen insulae, dorsal to the temporal pole. (37) This division may take place, however, anywhere between 1 and 4 cm from its origin from the internal carotid artery, and this point may be different on each hemisphere of the same brain. (36)

The pattern of arborization of this artery on the cortical surface consists of a bifurcation (78% of hemispheres), trifurcation (12%), or division into multiple trunks (10%). (38)

The anterior temporal branch irrigates the temporal pole and a variable extent of the lateral temporal lobe. It originates as part of a trifurcation of the middle cerebral artery or in a common trunk with the orbitofrontal artery that distributes over the inferior and middle frontal gyri and the orbital surface of the frontal lobe. The prefrontal and precentral arteries cover two triangular-shaped areas of the frontal lobe with vertices toward the temporal pole, situated between the frontal pole and the precentral gyrus. The rolandic arteries supply the precentral and postcentral gyri. The angular artery runs caudally over the superior temporal gyrus and reaches the occipital lobe.

The cortical branches of the middle cerebral artery anastomose with branches of the anterior cerebral artery and posterior cerebral artery. (Figure 5) The region over which these anastomosis occur has been diagramatically represented as a large diameter circle.

This area is considered of clinical significance because it appears to be the site of "watershed" infarctions. (37)

The anterior choroidal artery (ach) branches out of the posterior wall of the internal carotid artery proximal to the origin of the middle cerebral artery and anterior cerebral artery and distal to the posterior cerebral-internal carotid anastomosis. (Figure 3)

The first branches from this vessel supply the amygdala and the rostral hippocampus. The anterior choroidal then continues caudally giving branches that irrigate the rest of the hippocampus, optic tract, the tail of the nucleus caudatus, medial pallidum, ventral thalamus, the posterior limb of the internal capsule, and lateral geniculate. The vessel then proceeds caudolaterally giving numerous branches to the choroid plexus of the temporal horn of the lateral ventricle.

The anterior choroidal artery anastomoses with branches of the anterior cerebral artery, posterior cerebral artery, and middle cerebral artery.

2.3 Vertebrobasilar System

The vertebral arteries run together to form the basilar artery (Figure 3) which starts its course over the ventral portion of the medulla, usually at or a few millimeters below the inferior border of the clivus. The anterior spinal artery (aspa) originates from both vertebral arteries, close to the point where they join, or occasionally from only one of them. (Figure 3)

The remaining medial branches of the intracranial portion of the vertebral artery supply the anterior medulla and pyramids. The lateral branches of this portion include the posterior inferior cerebellar artery (pica) and branches to the inferior cerebellar peduncle, lateral medulla and the inferior olive and associated structures. The pica, which may alternatively originate from the basilar or from the extracranial portion of the vertebral, irrigates the inferolateral cerebellar hemisphere. (Figure 2) The extent

of the cerebellar distribution of the pica is variable and inversely related to the size of the territory covered by the anterior inferior cerebellar artery (aica), a branch of the basilar artery.

On its course toward the cerebellum, the pica gives branches to the lower medulla and fourth ventricle.Blood flow in the basilar artery is laminar, as in practically all normal arteries in the body with the possible exception of the root of the aorta during the ejection phase. (39)

Numerous branches, called perforator arteries because they penetrate the substance of the brainstem, originate from the basilar artery along its course. (Figure 6 – Figure 7) Median perforators (mper) originate from the posterior wall of the basilar and penetrate the pons and midbrain to irrigate structures near the midline, reaching the floor of the fourth ventricle.
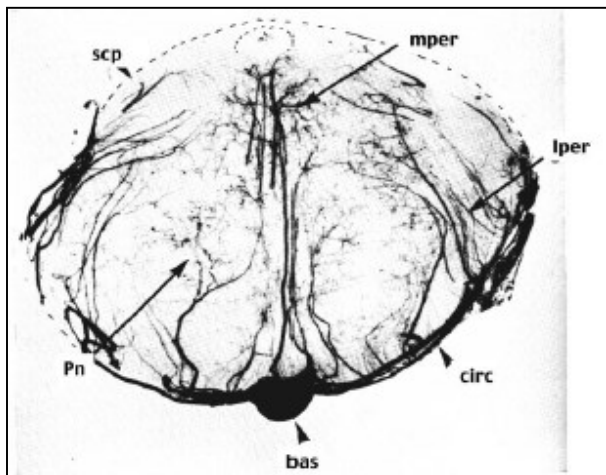

Figure 6 - Angiography of the pons (rostral end) shown in a coronal section. Pn, pontine nucleus; scp, superior cerebellar peduncle. Arteries abbrevations: bas, basilar; mper, median perforators; lper, lateral perforators; circ, pontine circumflex.
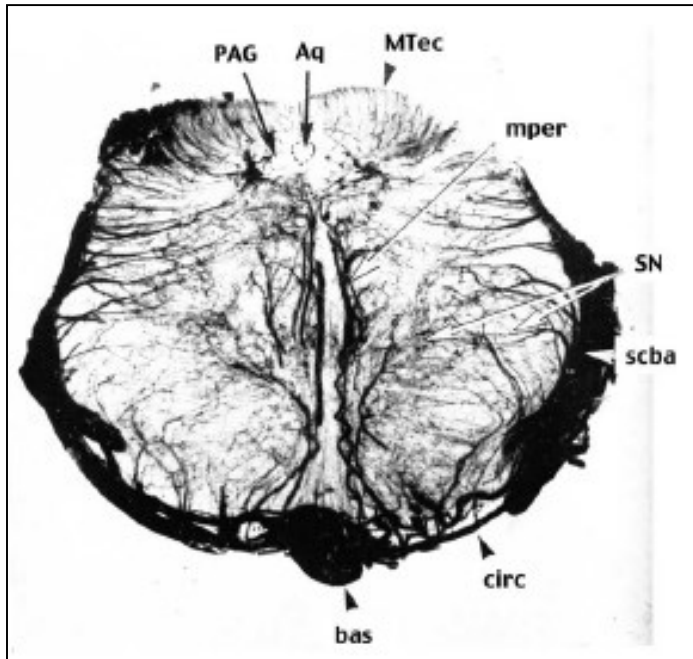
Figure 7 - Angiography of the mesencephalon (caudal end) shown in a coronal section. PAG, periacqueductal gray; Aq, cerebral acqueduct; MTec, mesencephalic tectum; SN, substantia nigra. Arteries abbrevations: bas, basilar; mper, median perforators; scba, superior cerebellar; circ, mesencphalic circumflex.

The aica originates from the basilar as a single vessel or as several smaller twigs (Figure 2). It corse caudolaterally and provides several perforators to the pons before it reaches the inferior surface of the cerebellar hemisphere. (Figure 8)

Its area of distribution, as stated previously, depends on the size of the territory of the pica.

The superior cerebellar artery (scba) arises at or just caudal to the rostral division of the basilar into the two posterior cerebral arteries. (Figure 2) A large perforator arises from this artery at its origin or sometimes from the basilar, and a number of smaller perforators originate from the superior cerebellar artery and distribuite to the pontine lateral tegmental region.

There are usually three cerebellar branches of the scba: the medial, distributing mostly over the vermis, and the intermediate and lateral, over the cerebellar hemispheres. (Figure 8) (40)

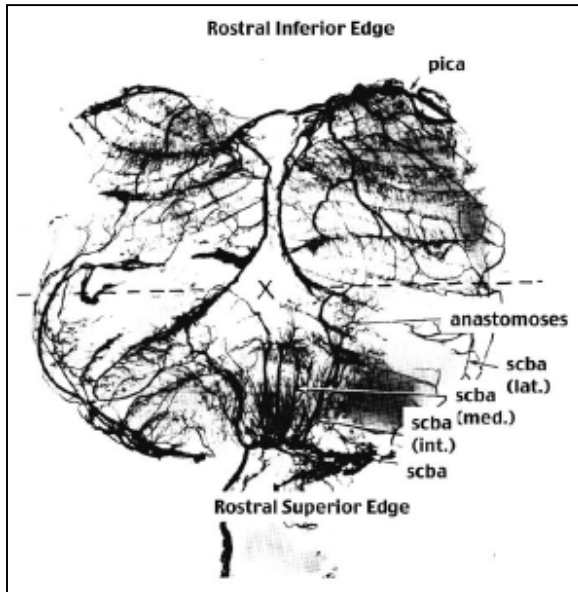**Figure 8** - Postmortem angiogram in which the entire cerbellar cortex has been flattened to show the multiple anastomoses between the territories of the superior cerebellar (scba) and the posterior inferior cerebellar (pica) arteries. The lateral (lat.), intermediate (int.) and medial (med.) branches of the scba are shown. The rostral inferior edge of the cerebellum is at the top and the rostral superior edge at the bottom of the figure. The line labeled "X" represents the most caudal edge of the cerebellar cortex.

The basilar artery terminates dividing into two posterior cerebral arteries, which connect with the posterior communicating arteries (pcoma) and then curve around the midbrain. At this level, their position is usually superomedial to the tentorium and they terminate in a number of cortical vessels over the calcarine fissure. (Figure 3) Three segments are commonly described in the posterior cerebral artery: P1 from its origin until the anastomosis with the posterior communicating, P2 from the end of P1 to the back of the midbrain, and P3 as the segment running through the lateral portion of the quadrigeminal cistern. (41)

The medial posterior choroidal artery (Figure 2) originates from the P2 segment and courses around the brainstem giving off branches contributing to the irrigation of the midbrain, tectal plate, pineal gland, posterior thalamus, habenula, and medial geniculate body. It also supplies the homolateral choroid plexus of the third ventricle. (40)

Lateral to the medial posterior choroidal artery originate a number of lateral posterior choroidal arteries, up to nine per side. These vessels supply parts of the midbrain crus, the pineal body, splenium, posterior commissure, tail of the caudate nucleus, thalamus, and fornix. They enter the lateral ventricle where they supply the choroid plexus and then enter the foramen of Monro to anastomose with the medial posterior choroidal arteries. (41)

The cortical branches of the posterior cerebral artery are the more distal to the origin of this artery and distribute to the inferior and medial surface of the temporal lobe (anterior and posterior temporal branches) and to the medial aspect of the occipital lobe and posterior parietal lobe (calcarine and parietooccipitalbranches). Arteries at the edge of the posterior cerebral artery territory anastomose with the terminal arborizations of the middle cerebral and anterior cerebral arteries. (Figure 5)

2.4 The Arterial Circle

One of the notable characteristics of cerebrovascular anatomy is the abundance of anastomoses between large arteries, extracranially (angular to ophthalmic arteries) and intracranially (the arterial circle at the base of the brain) as well as between small arteries on the surface of the brain (the leptomeningeal plexus). (Figure 9) (42)
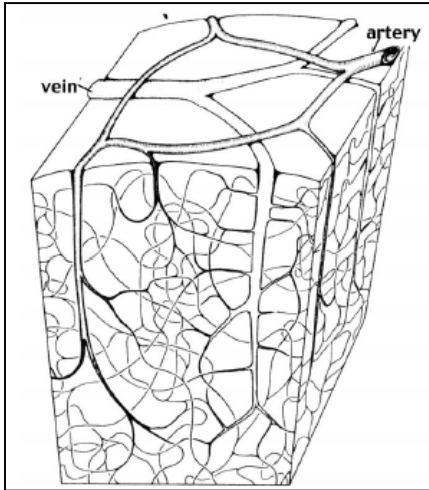
Figure 9 – Schematic three-dimensional representation of the cerebral cortex vascular architecture. Arteries and veins run at a distance and connect at all levels through capillary loops inside the cortex. Small arterial circles join the cortical arteries giving origin to multiple perforators

Johan Vesling (1595–1649), from the School of Padua and the anatomist Johan Wepfer (1620–1695) also described the arterial circle.

Thomas Willis, Sedleian Professor of Natural Philosophy at Oxford, was also aware of this feature and asked his friend Christopher Wren, the architect of Canterbury Cathedral, to illustrate the arterial circle which he did masterfully. The image is somewhat idealized (Figure 3, *top right*) because all vessels appear symmetrical and with almost the same diameter, a condition that is indeed rare in the adult human brain. (43)

In 1947, Padget (1944) summarized the findings of a large number of anatomical specimens reported in the literature at the time. Starting with a "typical" circle with the anterior communicating as half to two thirds the size of the anterior cerebral, in turn half the size of the internal carotid, and the pcoma with half the size of the posterior cerebral, in turn half the size of the basilar, agreement of the posterior portion of the circle (posterior communicating and posterior cerebral arteries) with this pattern was found in less than 50% of 1033 cases. The anterior portion of the

circle (anterior cerebral and anterior communicating arteries) was considered to be more dependable than the posterior one as a source of collateral circulation, although no quantitative data was presented to support this statement.

Quantitative estimates of the prevalence of circle anomalies in 994 specimens indicate that a complete "typical" circle is found in only 20% of cases. (37)

Anomalies included absence or hypoplasia of the anterior communicating artery (20%), posterior communicating arteries on one or both sides (38%), and proximal anterior cerebral artery (12%). The rest of the anomalies were represented by hypoplasia of the divisional branches of the basilar artery.

A serious limitation of the anatomical studies is that although they can identify cases of anatomical compromise of collateral circulation through the arterial circle when some of its component vessels are severely hypoplastic or absent, they cannot ascertain whether a vessel of "normal" caliber would be able to sustain a significant amount of additional blood flow to compensate for stenosis or occlusion of one or more of the circle-supplying vessels.

The ability of the posterior communicating artery to supply collateral blood flow, for instance, has been found to depend not only on its diameter but also on the resistance of its afferent and efferent vessels. (42)

IAA and MRA can provide information on direction of flow in the component vessels of the circle in addition to the anatomical information. However, the transcranial color-coded duplex ultrasonography technique (TCCD) can provide currently the most accurate information regarding blood velocity (although not volumetric blood flow due to lack of vessel cross-sectional area information) in the blood vessels that supply the brain.

It is important to note that in the presence of anatomically complete arterial circle, blood velocity in the homolateral middle cerebral artery decreased between 25% and 67% during brief unilateral carotid compression. In this context, it is important to note that failure of adequate collateral blood flow compensation during sudden unilateral internal carotid occlusion, defined as a decrease of middle cerebral artery blood velocity > 40%, has been reported to be followed by hemodynamic cerebral infarction if the occlusion becomes permanent. (43)

2.5 Microvascular Anatomy

The diagram shown in Figure 9 illustrates the existence of a network of anastomosing pial arteries (the leptomeningeal plexus) from which penetrating vessels emerge at right angles, capillarize and drain into collecting veins that course to the pial surface widely separated from the supplying arteries. The detailed anatomy of the intervening capillary plexus is extremely complex and highly dependent on the neuronal anatomy, to the extent that observation of the blood vessel network allows sometimes to recognize the underlying neuronal substrate. Detailed analysis of the intracortical vascular network reveals arterioles that traverse all cortical layers with minimal or no branching to reach the deeper layers and the subcortical white matter, where they give off capillaries that orient themselves in compliance with the general trajectories of nerve fibers.

Other groups of arteries give branches to subcortical and cortical levels (Figure 10, A5) all cortical levels (Figure 10, A4) or restricted cortical layers. (Figure 10, A1-A3) In most areas of the cortex, many arteries converge over a single intracortical vein that are less numerous than arteries and of a larger caliber, with their afferent vessels

joining at right angles (Figure 10, V4 - V5). (42)

Vascular Territories

A large number of descriptions of the territories covered by the various cerebral arteries are available in the literature. The line of separation between the territories of the anterior cerebral artery, middle cerebral artery, and posterior cerebral artery, for instance, depend on the hemodynamic conditions in each territory that determine the extent to which the three main supplying vessels contribute to their irrigation. Thus, proximal occlusion of the middle cerebral artery may induce the anterior cerebral artery and posterior cerebral artery territories to expand over that of the middle cerebral artery. Another condition of a shift in distribution of arterial supply may be found as described earlier with a high-flow arteriovenous malformation that would create a "sump" effect drawing blood from arteries of neighboring territories. (42)
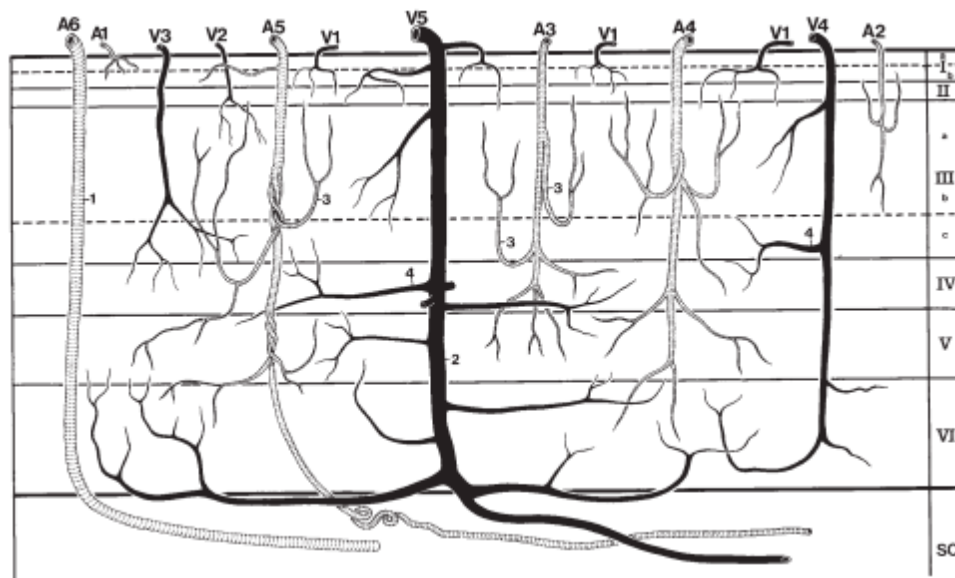
Figure 10 – Schematic two-dimensional representation of the types of arteries and veins found in the cerebral cortex. Arteries distribute to the superficial layers only (A1, A2), to layers I-V (A3), to all layers (A4, A5), or preferentially to the subjacent white matter (A6). This segmental arrangement creates the anatomical substrate for a differential control of blood flow to cortical layers. Veins (shown in solid balck) are usually larger and receive afferent branches at right angles from circumscribed (V1-V3) or wide (V4, V5) distributions. I-VI, cortical layers; SC, subcortical white matter.

Chapter 3

Doppler Analysis Ultrasound of Fetal Circulation in normal pregnancy

In the last twenty years the capacity of ultrasound flow imaging have really increased.

Color flow imaging is now ordinary and facilities such as 'Power' or 'Energy' Doppler provide new ways of imaging flow.

With such versatility, it is tempting to employ the technique for ever more demanding applications and to try to measure increasingly subtle changes in the maternal and fetal circulations.

34

3.1 Basic Principles

Ultrasound images of flow, whether Color flow or spectral Doppler, are obtained from measurements of movements.

In ultrasound scanners, a series of pulses is transmitted to detect movement of blood. Echoes from moving scatterers exhibit slight differences in the time for the signal to be returned to the receiver. (Figure 1)

These differences can be measured as a direct time difference or, more usually, in terms of a phase shift from which the 'Doppler frequency' is obtained (Figure 2). They are processed to produce either a color flow display or a Doppler sonogram.
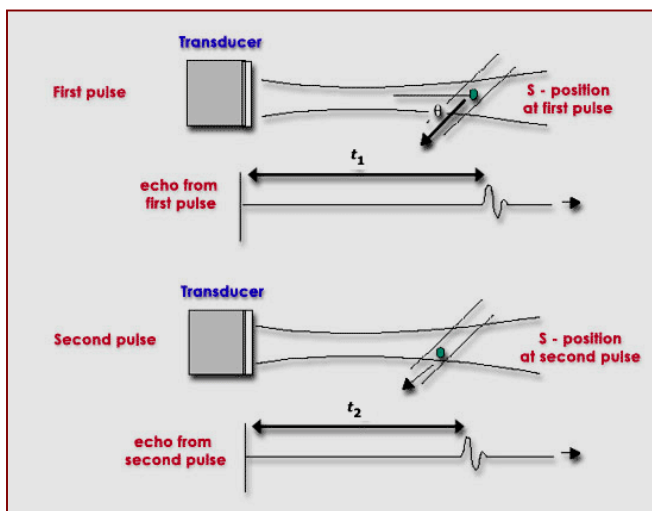
Figure 1 - Ultrasound velocity measurement. The diagram shows a scatterer S moving at velocity V with a beam/flow angle φ. The velocity can be calculated by the difference in transmit-to-receive time from the first pulse to the second (t2), as the scatterer moves through the beam.
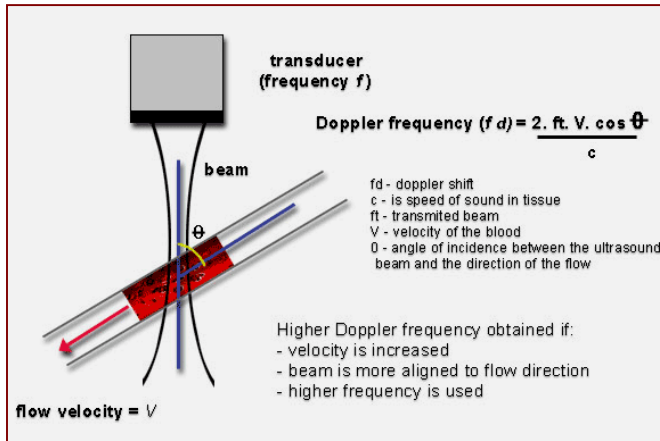
Figure 2 - Doppler ultrasound. Doppler ultrasound measures the movement of the scatterers through the beam as a phase change in the received signal. The resulting Doppler frequency can be used to measure velocity if the beam/flow angle is known. There has to be motion in the direction of the beam in fact if the flow is perpendicular to the beam, there is no relative motion from pulse to pulse.

The size of the Doppler signal is dependent on:

(1) Blood velocity: as velocity increases, so does the Doppler frequency;

(2) Ultrasound frequency: higher ultrasound frequencies give increased Doppler frequency. As in B-mode, lower ultrasound frequencies have better penetration.

(3) The choice of frequency is a compromise between better sensitivity to flow or better penetration;

(4) The angle of insonation: the Doppler frequency increases as the Doppler ultrasound beam becomes more aligned to the flow direction (the angle φ between the beam and the direction of flow becomes smaller). (Figure 3) (44, 45)
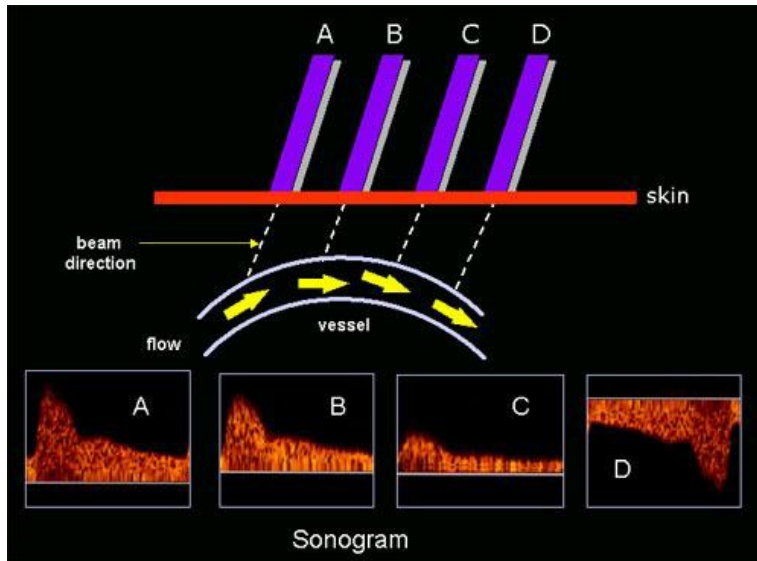
Figure 3 - Effect of the Doppler angle in the sonogram. (A) higher-frequency Doppler signal is obtained if the beam is aligned more to the direction of flow. In the diagram, beam (A) is more aligned than (B) and produces higher-frequency Doppler signals. The beam/flow angle at (C) is almost 90° and there is a very poor Doppler signal. The flow at (D) is away from the beam and there is a negative signal.

Methodology of Doppler assessment of the placental and fetal circulations

Doppler ultrasound provides a non-invasive method for the study of fetal hemodynamics and umbilical arteries gives information on the perfusion of the uteroplacental and fetoplacental circulations, respectively, while Doppler studies of selected fetal organs are valuable in detecting the hemodynamic rearrangements that occur in response to fetal hypoxemia.

3.2 Uteroplacental Circulation

Anatomy

The blood supply to the uterus comes mainly from the uterine arteries with a small contribution from the ovarian arteries. These vessels anastomose at the cornu of the

uterus and give rise to arcuate arteries that run circumferentially around the uterus. The radial arteries arise from the arcuate vessels and penetrate at right angles into the outer third of the myometrium. These vessels then give rise to the basal and spiral arteries, which nourish the myometrium and decidua and the intervillous space of the placenta during pregnancy, respectively. (46, 47, 48)

3.3 Physiological changes in pregnancy

Physiological modification of spiral arteries is required to permit the increase in uterine blood flow which is necessary to satisfy the respiratory and nutritional requirements of the fetus and placenta.

The conversion of the spiral arteries to uteroplacental arteries is termed *'physiological change'*. It occurs in two stages: the first wave of trophoblastic invasion converts the decidual segments of the spiral arteries in the first trimester and the second wave converts the myometrial segments in the second trimester. (49) As a result of this *'physiological change'*, the diameter of the spiral arteries increases from 15–20 to 300–500 mm, reducing impedance to flow and optimizing fetomaternal exchange in the intervillous space.

Uterine artery

Schulman described the use of continuous wave Doppler ultrasound to identify the uterine artery. The Doppler probe was directed into the parauterine area in the region of the lower uterine segment and rotated until a characteristic waveform pattern was obatined.

The patterns of uterine, arcuate and iliac vessels could be differentiated from each

other and from other vessels in the pelvis. The presence of an early diastolic notch was noted and was found to disappear between 20 and 26 weeks.

Arduini compared color flow imaging and conventional pulsed Doppler in the study of the uterine artery. (50)

Color flow imaging was used to visualize the flow through the main uterine artery medial to the external iliac artery and the Doppler sample gate was placed at the point of maximal color brightness. Color flow imaging was found to allow a higher number of reliable recordings to be obtained, to shorten the observation time and to reduce the intra and interobserver coefficients of variation. (Figure 4) (51)
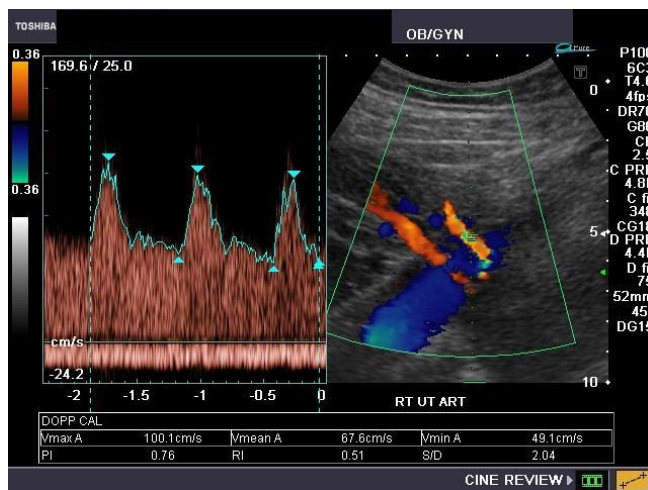
Figure 4 - Ultrasound image with conventional color Doppler showing the uterine artery and the external iliac artery. Normal flow velocity waveforms from the uterine artery at 24 weeks of gestation demonstrating high diastolic flow.

Impedance to flow in the uterine arteries decreases with gestation. The initial fall until 24–26 weeks is thought to be due to trophoblastic invasion of the spiral arteries, but a continuing fall in impedance may be explained by a persisting hormonal effect on elasticity of arterial walls. Impedance in the uterine artery on the same site as the placenta is lower, which is thought to be due to the trophoblastic invasion only taking place in placental spiral arteries and the fall in impedance engendered by this being

transmitted to other parts of the uterine circulation through collaterals. The intra- and interobserver coefficients of variation in the measurement of impedance to flow from the uterine arteries are both 5–10%. (Figure 5) (50)
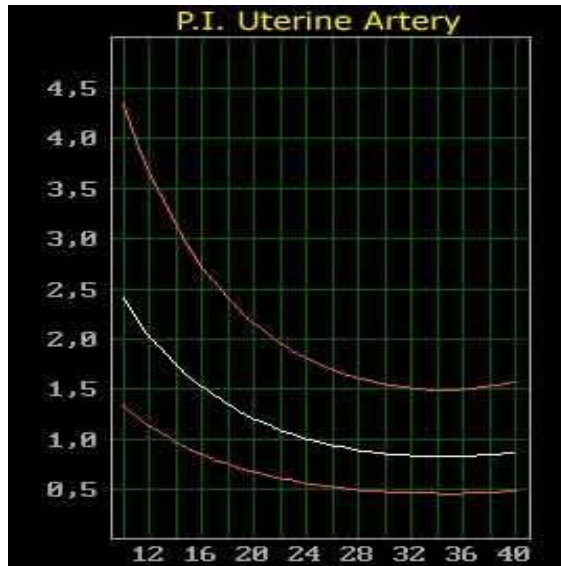
Fig 5 - Pulsatility index (PI) in the uterine artery with the gestation (mean, 95th and 5th centiles).

Umbilical artery

The umbilical artery was the first fetal vessel to be evaluated by Doppler velocimetry. Flow velocity waveforms from the umbilical cord have a characteristic saw-tooth appearance of arterial flow in one direction and continuous umbilical venous blood flow in the other. Continuous wave Doppler examination is simple. The transducer is manipulated to obtain the characteristic waveforms from the umbilical artery and vein. With a pulsed wave Doppler system, an ultrasound scan is first carried out, a free-floating portion of the cord is identified and the Doppler sample volume is placed over an artery and the vein (Figure 6) (51)
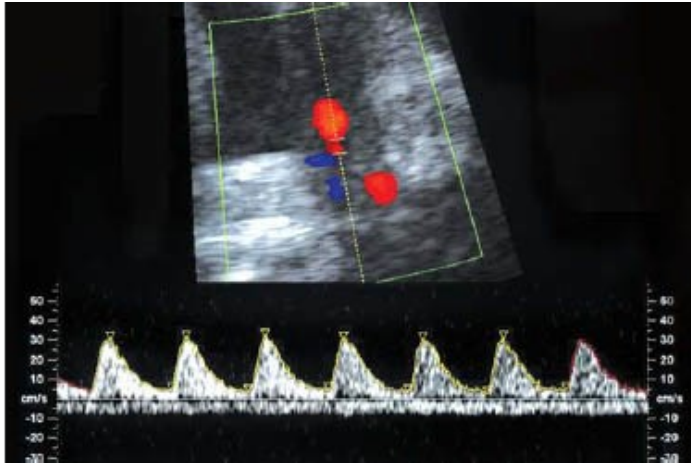
Figure 6 - Ultrasound image with color Doppler showing the umbilical cord, red umbilical artery and blue umbilical vein (left). Normal flow velocity waveforms from the umbilical vein (bottom) and artery (top) at 32 weeks of gestation.

With advancing gestation, umbilical arterial Doppler waveforms demonstrate a progressive rise in the end-diastolic velocity and a decrease in the impedance indices. (Figure 7)
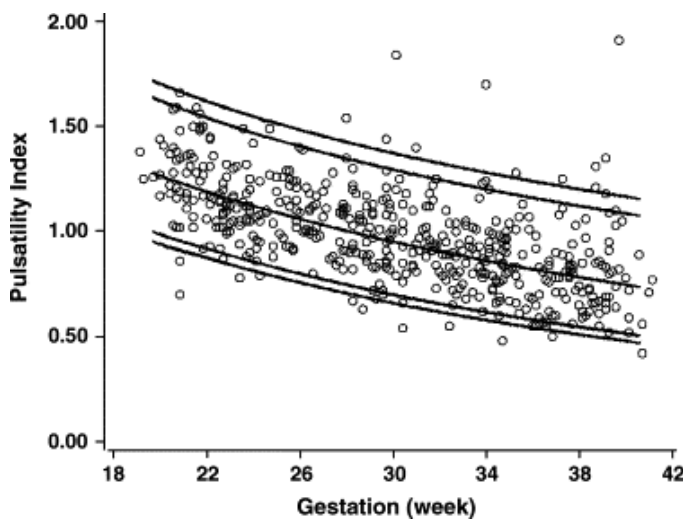
Figure 7 - Pulsatility index (PI) in the umbilical artery with the gestation (mean, 95th and 5th centiles).

Human placental studies have demonstrated that there is continuing expansion of the fetoplacental vascular system throughout the pregnancy. Furthermore, the villous vascular system undergoes a transformation, resulting in the appearance of sinusoidal

dilatation in the terminal villous capillaries as pregnancy approaches term, and more than 50% of the stromal volume may be vascularized.

The intra- and interobserver variations in the various indices are about 5% and 10%, respectively. (50)

Cerebral Arteries

With the color Doppler technique, it is possible to investigate the main cerebral arteries such as the internal carotid artery, the middle cerebral artery, the anterior and the posterior cerebral arteries and to evaluate the vascular resistances in different areas supplied by these vessels.

A transverse view of the fetal brain is obtained at the level of the biparietal diameter. The transducer is then moved towards the base of the skull at the level of the lesser wing of the sphenoid bone. Using color flow imaging, the middle cerebral artery can be seen as a major lateral branch of the circle of Willis, running anterolaterally at the borderline between the anterior and the middle cerebral fossae. (Figure 8) (52)
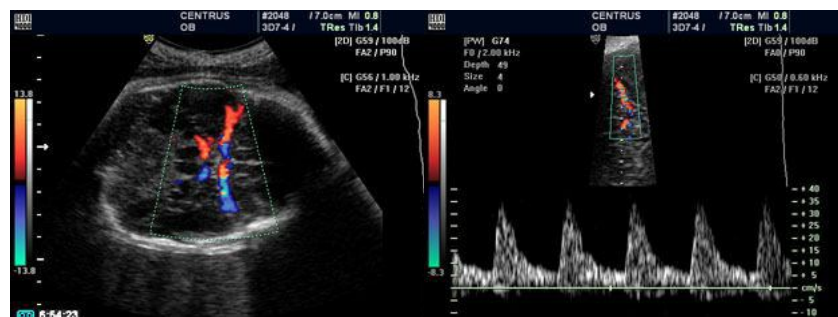
Figure 8 - Transverse view of the fetal head with color Doppler showing the circle of Willis (left). Flow velocity waveforms from the middle cerebral artery at 32 weeks of gestation (right).

The pulsed Doppler sample gate should be placed on the middle portion of this vessel to obtain flow velocity waveforms. Due to the course of this blood vessel, it is almost always possible to obtain an angle of insonation which is less than 10°. During the

studies, care should be taken to apply minimal pressure to the maternal abdomen with the transducer, as fetal head compression is associated with alterations of intracranial arterial waveforms.

In healthy fetuses, impedance to flow in the fetal aorta does not change with gestation during the second and early third trimesters of pregnancy, but it subsequently decreases. (Figure 9) (48)
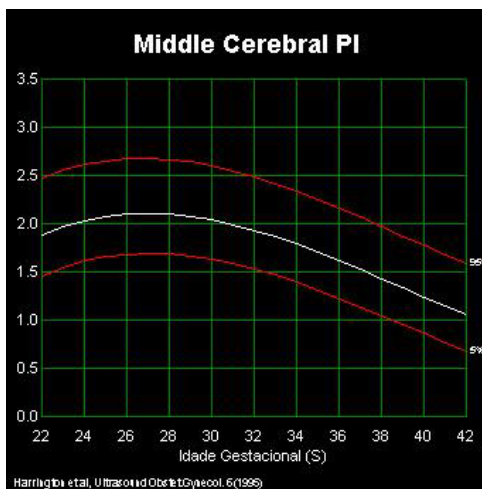
Figure 9 - Pulsatility index (PI) in the middle cerebral artery with the gestation (mean, 95th and 5th centiles).

Ductus venosus

The ductus venosus plays a central role in the return of venous blood from the placenta: well-oxygenated blood flows directly towards the heart. Approximately 40% of umbilical vein blood enters the ductus venosus and accounts for 98% of blood flow through the ductus venosus, because portal blood is directed almost exclusively to the right lobe of the liver. (48)

The typical waveform for blood flow in venous vessels consists of three phases. The highest pressure gradient between the venous vessels and the right atrium occurs during ventricular systole (S), which results in the highest blood flow velocities

43

towards the fetal heart during that part of the cardiac cycle. Early diastole (D), with the opening of the atrioventricular valves and passive early filling of the ventricles (E-wave of the biphasic atrioventricular flow waveform), is associated with a second peak of forward flow. The nadir of flow velocities coincides with atrial contraction (a) during late diastole (A-wave of the atrioventricular flow waveform). During atrial contraction, the foramen ovale flap and the crista dividens meet, thereby preventing direct blood flow from the ductus venosus to the left atrium during that short period of closure of the foramen ovale. (Figure 10) (51)
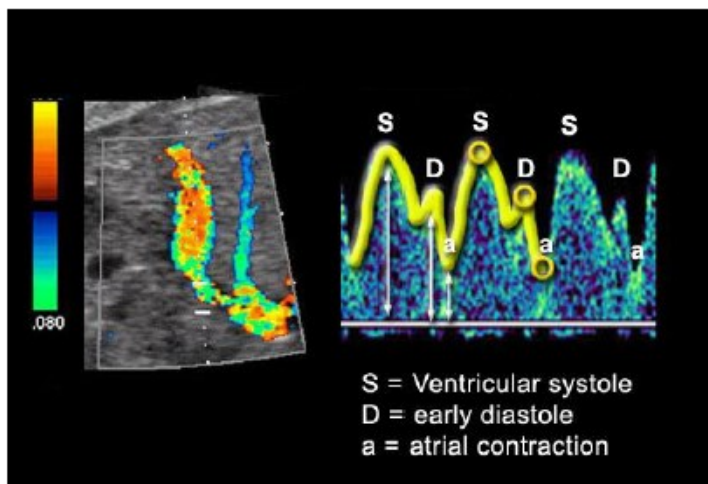
Figure 10 - Normal flow velocity waveform of the ductus venosus. The first peak indicates systole, the second early diastole and the nadir of the waveform occours during atrial contraction.

Chapter 4

Doppler Analysis Ultrasound of Fetal Circulation in Fetal Growth Restriction

4.1 Bidimensional Doppler Assessment of the Fetus with Fetal Growth Restriction

The condition of Intra Uterine Growth Retardation (IUGR) or Fetal Growth Restriction (FGR) is defined as sonographic estimated fetal weight < 10th percentile for gestational age. (53, 54)

According to the American College of Obstetricians and Gynecologists, FGR is "one of the most common and complex problems in modern obstetrics".

This characterization is understandable considering the various published definitions, poor detection rate, limited preventive or treatment options, multiple associated morbidities and increased likelihood of perinatal mortality associated with FGR. Suboptimal growth at birth is linked with impaired intellectual performance and diseases such as hypertension and obesity in adulthood. (55, 56)

Current challenges in the clinical management of FGR include accurate diagnosis of the truly growth-restricted fetus, selection of appropriate fetal surveillance and optimizing the timing of delivery.

Despite the potential for a complicated course, antenatal detection of FGR and its antepartum surveillance can improve outcomes. (57)

We acknowledge that defining small for gestational age (SGA) (birthweight < 10th percentile for gestational age) by general population charts vs customized charts is an important issue. (54, 56)

Pathological findings in FGR Fetuses

Fetal growth restriction is associated with an inadequate quality and quantity of maternal vascular response to placentation.

In this condition, there are characteristic pathological findings in the placental bed.

Uterine arteries

In pregnancies complicated by fetal growth restriction, impedance to flow in the uterine arteries is increased. (Figure 1) (58)

Studies in women with hypertensive disease of pregnancy have reported that, in those with increased impedance (increased resistance index or the presence of an early diastolic notch), compared to hypertensive women with normal flow velocity waveforms, there is a higher incidence of pre-eclampsia, intrauterine growth restriction, emergency Cesarean delivery, placental abruption, shorter duration of pregnancy and poorer neonatal out come. (49)
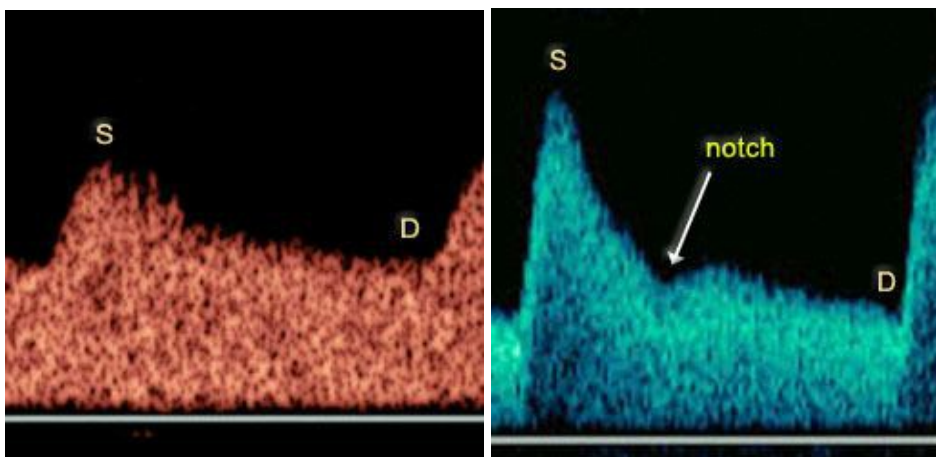
Figure 1 - Normal (left) and abnormal (right) flow velocity waveforms from the uterine arteries at 24 weeks of gestation. (S= peak systolic; D= End diastolic)

Umbilical artery Doppler

Doppler velocimetry of the umbilical artery assesses the resistance to blood perfusion of the fetoplacental unit (Figure 20). As early as 14 weeks, low impedance in the umbilical artery permits continuous forward flow throught the cardiac cycle. (59, 60) Maternal or placental conditions that obliterate small muscular arteries in the placental tertiary stem villi result in a progressive decrease in end-diastolic flow in the umbilical artery Doppler waveform until absent (Figure 21) and then reversed (Figure 22) flow during diastole are evident. (61)

Reversed end-diastolic flow in the umbilical arterial circulation represents an advanced stage of placental compromise and has been associated with obliteration > 70% of arteries in placental tertiary villi. (57)

Absent or reversed end-diastolic flow in the umbilical artery is commonly associated with severe (birthweight < 3rd percetile for gestational age) FGR and oligohydramnios. (62)

Althought there are other quantitative assessments of umbilical artery Doppler (eg. Resistance index) available, the systolic to diastolic (S/D) ratio and pulsatility index are commonly used and either may be sufficient to manage most cases of suspected FGR. When end-diastolic flow is absent, the S/D ratio is immeasurable and PI may be used.

In clinical practice, Doppler waveforms of the umbilical artery can be obtained from any segment along the umbilical cord. Waveforms obtained near the placental end of the cord reflect downstream resistance and show higher and-diastolic velocity than waveforms obtained near the abdominal cord insertion.

To optimize reproducibility, we suggest interrogating the umbilical artery at the abdominal cord insertion. The S/D ratio and PI should be obtained in the absence of fetal breathing and when the waveform is uniform. (57)

Fetal arterial blood flow redistribution

In fetal hypoxemia, there is an increase in the blood supply to the brain, myocardium and the adrenal glands and reduction in the perfusion of the kidneys, gastrointestinal tract and the lower extremities. Although knowledge of the factors governing circulatory readjustments and their mechanism of action is incomplete, it appears that partial pressures of oxygen and carbon dioxide play a role, presumably through their action on chemoreceptors. This mechanism allows preferential redistribution of nutrients and oxygen to vital organs, thereby compensating for diminished placental resources. However, compensation through cerebral vasodilatation is limited and a plateau corresponding to a nadir of pulsatility index (PI) in cerebral vessels is reached at least 2 weeks before the development of the fetus is jeopardized. Consequently, arterial vessels are unsuitable for longitudinal monitoring of growth-restricted fetuses. Venous velocity waveforms give more information regarding fetal well-being or compromise. (57)

Middle cerebral artery

In the hypoxemic FGR fetuses, due to impaired placental perfusion, the Pulsatility Index (P.I.) in the umbilical artery is increased while in the fetal middle cerebral artery the PI is decreased; consequently, the ratio between the umbilical artery and middle

cerebral artery (UA/MCA), called cerebro − placental ratio (CPR), is increased. (Figure 2) (63, 64, 65)
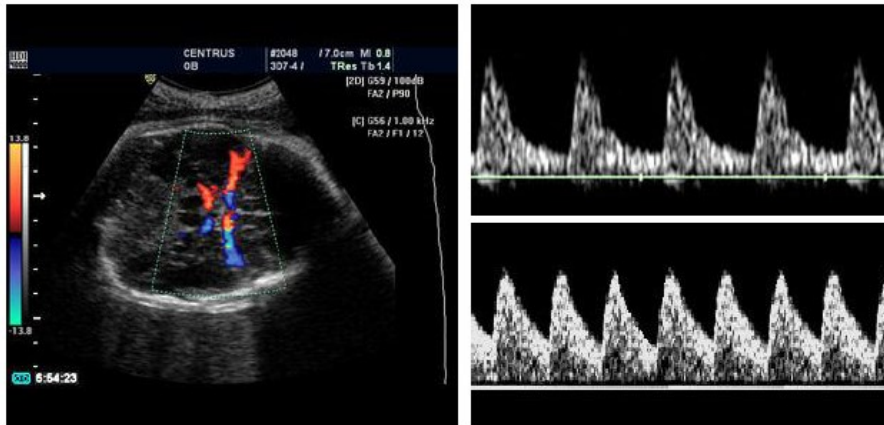
Figure 2 - Color Doppler examination of the circle of Willis (left). Flow velocity waveforms from the middle cerebral artery in a normal fetus with low diastolic velocities (right, top) and in a FRG fetus with high diastolic velocities (right, bottom).

Ductus venosus

In severe hypoxemia, there is redistribution in the umbilical venous blood towards the ductus venosus at the expense of hepatic blood flow. Consequently, the proportion of umbilical venous blood contributing to the fetal cardiac output is increased. There is a doubling of umbilical venous-derived oxygen delivery to the myocardium and an increase in oxygen delivery to the fetal brain.

In FGR fetuses there is an increase of reverse flow in the inferior vena cava during atrial contraction suggesting a higher pressure gradient in the right atrium.

The next step of the disease is the extension of the abnormal reversal of blood velocities in the inferior vena cava to the ductus venosus, inducing an increase of the S/A ratio, mainly due to a reduction of the A component of the velocity waveforms. (Figure 3) (66)
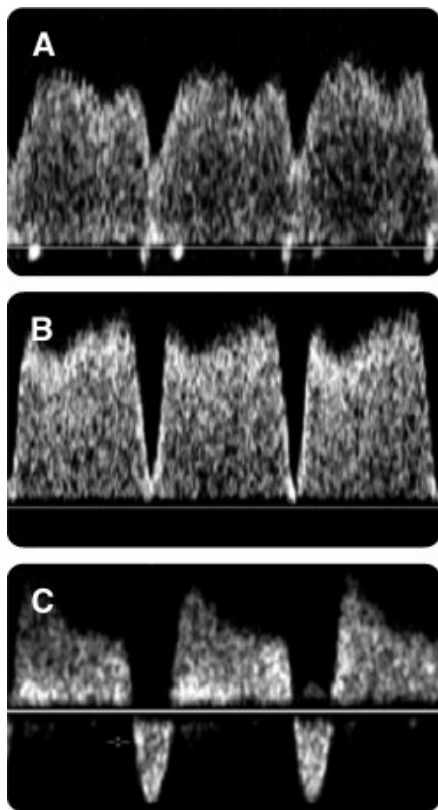
Figure 3 - Color Doppler examination of the ductus venosus with normal flow velocity waveforms (A). Abnormal waveform with revesal of flow during atrial contraction and markedly increased pulsatility in a FGR fetus (B, C).

Two different populations of fetuses affected by FGR had been identified according to the gestational week in which FGR had occured.

Early onset FGR fetuses, presenting before 34 gestational weeks, is associated with a progressive increase in blood flow resistance in the umbilical artery (UA), followed by a vasodilatation in the middle cerebral artery (MCA) and a deterioration in venous Doppler parameters and in the fetal biophysical score. UA end-diastolic velocity could became absent, or reversed, requiring preterm delivery.

Late onset FGR fetuses, presenting after 34 gestational weeks, is associated with mildly elevated, or even normal UA Doppler parameters and isolated cerebral vasodilation. (57)

Cerebral Placental Ratio (CPR)

The cerebroplacental ratio (CPR) is calculated as MCA-PI/UA-PI, offering the advantage of detecting the redistribution of blood flow earlier than the independent evaluation of both vessels.

Normal CPR values are above 1, meaning that MCA PI is higher than UA PI. However, when the process of brain vasodilatation begins, or the placental resistance increases, the CPR approaches 1. When the CPR is 1 or lower, there is a clear process of brain vasodilatation because the MCA PI is lower than the UA PI.

Consequently, the CPR can become abnormal when the UA-PI and MCA-PI are still within normal range. This characteristic becomes a disadvantage in early-onset IUGR fetuses with severe placental insufficiency as virtually all cases will show an abnormal CPR. Its clinical application seems to be orientated to late-onset IUGR fetuses with normal UA-PI. (67, 68)

4.2 Assessment of Fetal Brain Circulation in the management of FGR

Blood supply to the fetal brain is provided by the carotid and vertebral arterial systems forming the circle of Willis. After entering the fetal skull, each internal carotid artery gives two branches: the posterior communicating artery (PComA) and the anterior choroidal artery, then continuing with its terminal branches, the middle (MCA) and the anterior cerebral arteries (ACA).

The first segment of the ACA (ACA S1) reaches the midline, then continues towards the anterior wall of the skull as the ACA segment 2 (ACA S2), finishing as the pericallosal artery. The PComA plays a key role as a physiological hemodynamic shunt between the carotid and vertebral–basilar systems as it is connected with the

first segment of the posterior cerebral artery (PCA S1), which is the terminal branch of the vertebral system. From this point emerges the PCA segment 2 as a combination of both blood flow streams. (Figure 4) (57)
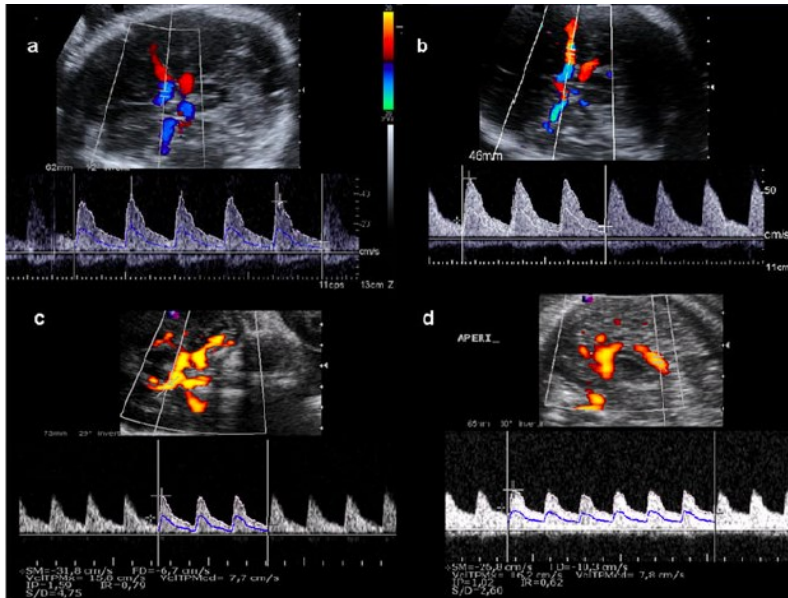
Figure 4 - Pulsed Doppler evaluation of the major fetal cerebral arteries: (a) anterior cerebral artery segment 1, (b) middle cerebral artery, (c) posterior cerebral artery segment 2, and (d) pericallosal artery

The vertebral arteries enter the brain through the foramen magna and joint in the middle forming the basilar artery, which runs in the midline of the brain stem until bifurcating in its two final branches, the left and right first segments of the PCA.

Application of the Doppler technique in the human fetus allows recognition and estimation of fetal blood flow and peripheral vascular impedance through the calculation of the pulsatility and resistance indices.

Original devices combined a linear real-time array and a fixed pulsed Doppler emitter. With the improvement of Doppler technology and the incorporation of color directional Doppler, it was possible to evaluate the complete intracranial circulation. Thus, the middle cerebral artery (MCA) became the first intracranial fetal vessel to be assessed, and is still considered as the clinical standard for the hemodynamic evaluation of the fetal brain. (69, 70)

Nevertheless, other arterial and venous territories have also been studied during the brain blood flow redistribution process.

Dubiel et al. suggested that in IUGR fetuses, the anterior cerebral artery might be affected earlier than the MCA. (71)

This concept was further explored by Figueroa-Diesel et al. who studied all major fetal cerebral arteries in IUGR fetuses at different stages of deterioration and found differences in their individual behavior.(28)

Benavides-Serralde et al. explored the MCA and two segments of the ACA at different stages of blood flow deterioration of the umbilical artery (UA) in IUGR fetuses, and found that both ACA segments presented earlier signs of vasodilatation than MCA. (72)

Although at early stages of fetal deterioration, the anterior and posterior cerebral arteries seemed to be already affected, MCA deteriorates later. Similarly, in a recent longitudinal study on term small for- gestational age (SGA) fetuses with normal UA Doppler, Cruz-Martinez et al. demonstrated that ACA pulsatility index (PI) becomes abnormal on average one week before abnormalities in the MCA can be detected. (73, 74)

Fractional Moving Blood Volume

A novel ultrasound derived technique termed fractional moving blood volume (FMBV) has been applied to indirectly evaluate changes in the fetal cerebral blood perfusion.

FMBV analyzes changes in amplitude (power) of the backscattered Doppler ultrasound signals originated from red blood cells. FMBV estimation aims to

compensate the effect that depth, tissue interfaces, and attenuation have on the PDU signals. (75, 76, 77, 78)

FMBV has been validated in experimental studies showing a high correlation with true blood flow changes and a good intraobserver and interobserver reliability.

In the fetal brain, four different regions of interest (ROI) have been explored, the frontal lobe, basal ganglia, complete midsagittal cerebral plane and posterior fossa (Figure 5); normal reference values throughout gestation for all regions are available in the literature. (75, 76)
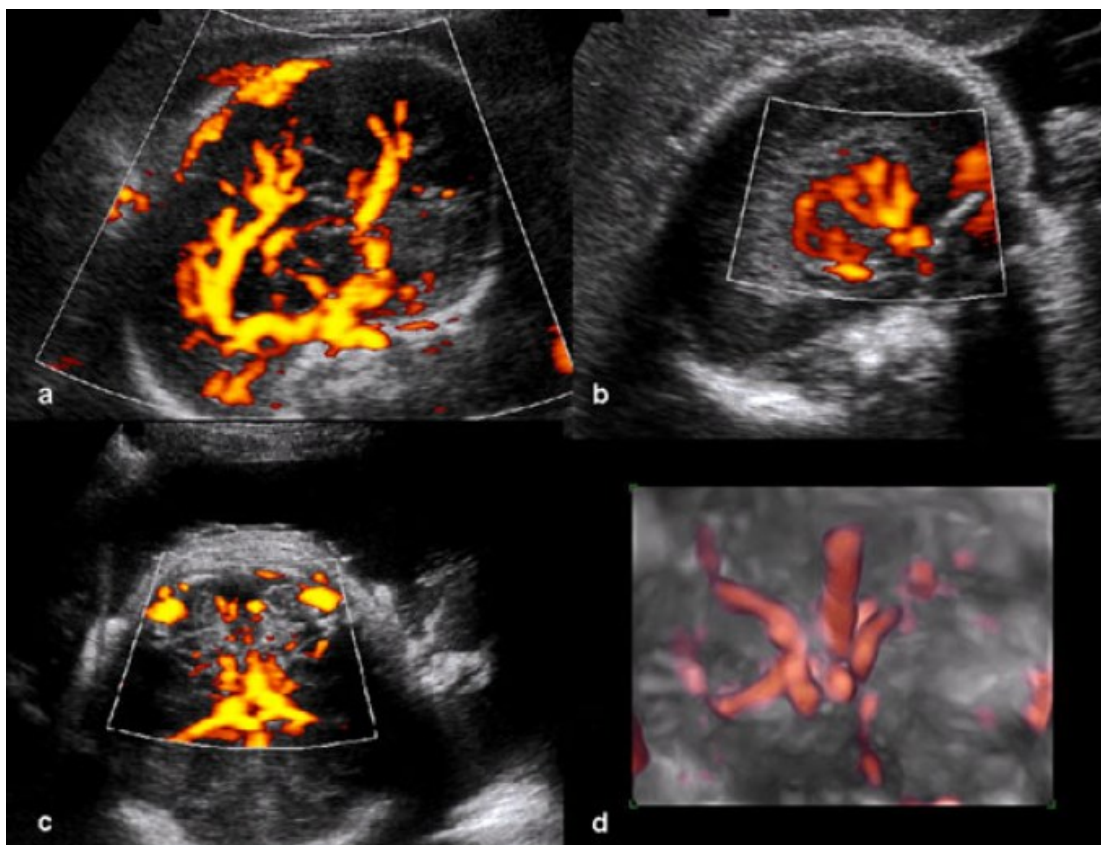
Figure 5 - Power Doppler evaluation of the fetal brain. (a) Midsaggital view of the complete brain and frontal lobe; (b) Basal ganglia obtained in a parasaggital view; (c) posterior fossa in a transverse view with the fetus facing down; (d) 3D power Doppler render of the arterial circle of Willis.

In normal fetuses, FMBV estimation is similar in all regions except the posterior fossa where the images are obtained through the occipital bone thus reducing the total

number of PDU signals reaching the US probe.

In mild IUGR affected fetuses, there is an increment in the blood flow perfusion to all cerebral regions with a preferential flow to the frontal lobe. As the IUGR fetus deteriorates, this perfusion pattern changes, increasing the blood flow towards the basal ganglia and decreasing it towards the frontal lobe. Recent research shows that this increased FMBV in the frontal lobe is already associated with altered neurodevelopment at birth. (79, 80)

Three – Dimensional Power Doppler Ultrasound

Three-dimensional ultrasound has been extensively used in obstetrics in order to visualize the body surface of the fetus, to obtain a volumetric analysis of fetal organs and placenta or to study the fetal morphology offline.

The fetal cerebral vascularization has been studied in the past using color and power Doppler, both with transabdominal and transvaginal probes, to evaluate haemodynamic changes in normal and complicated pregnancies or simply to study the morphology of the vascular tree of the fetal brain. The use of transvaginal Power Doppler, specifically, allows to detect very small vessels with extremely slow blood flow, such as medullary veins in the brain parenchyma.

Recently a new technology has enabled the study of blood flow in a sample volume. This new method is called 3D power Doppler (3DPD) ultrasound and it was introduced in obstetrics and gynecology in order to estimate semi-quantitative indices of vascularization and blood flow in the female pelvic organs, in the placenta and in fetal organs.

Three-dimensional power Doppler ultrasound (3D-PDU) has been recorded in the

fetal brain. 3D-PDU rendering is performed using the virtual organ computer-aided analysis (VOCAL™) technique applying a spherical tool for the delimitation of the ROI.

Three perfusion indices based on the voxel information of the PDU signals can be calculated within the rendered volume: the vascular index (VI, percentage of voxels in the volume), flow index (FI, mean voxel intensity in the volume) and vascular/flow index (VFI). (81)

The potential value of 3D-PDU indices is the calculation of blood perfusion in a volume of tissue, offering amore complete perspective of regional hemodynamic changes. Several reports on the fetal brain using 3D-PDU perfusion indices have been published confirming the increment in brain blood flow perfusion in IUGR fetuses. (82, 83, 84, 85)

The main limitations of applying 3D-PDU in the fetal brain are that, in order to construct the volume, the PDU signals must pass through different tissue interfaces, including the fetal skull.

Signals traveling through the fontanel will be brighter than signals passing through the skull. In addition, there is no method to compensate the effect that depth and brain tissue interfaces have on the PDU signals. This is not happening with FMBV, where acquisition of images is mainly performed through a region free of bone. Another limitation of 3D-PDU is the delineation of the region of interest.

The available reports apply the spherical virtual organ computer aided analysis tool to segment either, the complete fetal head or the circle of Willis; however, no specific landmarks have been proposed for the different cerebral segments. Using fundamental ultrasound for volume acquisition,

Benavides-Serralde et al. (2009) proposed specific landmarks for defining several fetal brain ROIs on 3D ultrasound volume files. (83)

4.3 Chronic Hypoxia and Brain Blood Flow Circulation

When fetal IUGR is suspected due to an estimated fetal weight <10th centile, or an abdominal circumference below 2 standard deviations, a complete Doppler evaluation must be performed.

This evaluation provides important information on the fetal hemodynamic adaptation to the hypoxic insult and on the fetal deterioration process thus optimizing the identification for the optimal time of delivery.

Previously, the Doppler fetal examination was applied stepwise starting with the umbilical artery and followed by the MCA.

This approach has been questioned as recent studies show that IUGR cases with normal flow in the umbilical artery might present signs of brain vasodilatation. These fetuses also show an increased risk for an abnormal neurodevelopment after birth. (86, 87, 88)

This evidence shows that the increment of blood flow to the fetal brain might be an early indicator of neurological damage, challenging the concept of a protective effect of the brain sparing mechanism. It is possible that the brain sparing effect might present two different components: an initially protective period followed by a stage of decompensation. Konje et al. reported that a late increment in the impedance indices is highly correlated with an increased risk of perinatal mortality, probably related to intracranial edema at the final stages of fetal Deterioration (Figure 8) (88)

Brain vascular parameter	Cut-off value	Clinical significance
ACA S1 PI	<5th percentile	Early marker of brain vasodilatation
	<5th percentile	Early marker of brain vasodilatation
MCA PI16,	<5th percentile	Late marker of brain vasodilatation
PCA PI	<5th percentile	Early marker of brain vasodilatation
MCA PSV /MCA PI	Normal/<5th percentile	Initial stages of brain vasodilatation
MCA PSV / ACM PI	Both <5th percentile	Advanced stages of brain vasodilatation
FMBV FRONTAL	>95th percentile	Initial stages of brain vasodilatation
FMBV BASAL GANGLIA	>95th percentile	Advanced stages of brain vasodilatation
3D-PDU	Increased	Brain vasodilatation

ACA, anterior cerebral artery; S1, segment 1; S2, segment 2; PI, pulsatility index, MCA, middle cerebral artery, PCA, posterior cerebral artery; PSV, peak systolic velocity; FMBV, fractional moving blood volume; 3D-PDU, three-dimmentional power Doppler ultrasound.

Fig 8 –Clinical significance of alterated fetal brain Doppler parameters

Nonetheless, this sign appears late and cannot be used for clinical follow up as it is a marker of brain hemodynamic claudication.

When present, it must be considered for an urgent delivery. In cases followed prospectively, other parameters must be first considered for identifying the moment when the protective sparing mechanism is lost. The anterior cerebral artery and the placental cerebral ratio seem to identify cases at earlier stages of deterioration. (89, 90, 91)

Additionally, evaluation of the waveform velocities might also contribute in identifying the moment when the protective brain sparing effect is lost. This precise moment is still unknown but the longitudinal evaluation of several vascular territories might help to define when the brain vascular system loses its adaptive mechanism increasing the risk for neurological damage.

In severe and early IUGR affected fetuses, the main objective of the fetal surveillance is to identify the best moment for delivery balancing neonatal and fetal morbidity and

mortality, when reasonable neonatal survival is achieved, the decision to deliver should be taken.

Evaluation of the fetal cerebral circulation must be part of the routine clinical follow up of early-onset IUGR; however, only in a small proportion of cases it can be independently used for the clinical decision to delivery. Other Doppler parameters, such as ductus venosus PI and the absence or reversed diastolic flow in the umbilical artery, are generally considered for this clinical decision. (92, 93)

It must be assumed that in early-onset IUGR fetuses, almost all cases already have brain vasodilatation increasing the risk of abnormal neuroadaptation or neurodevelopment after birth. In such cases, the aim of the fetal cerebral evaluation is to identify acute signs of intracranial edema that could orientate the clinical decision for delivery. After 32 weeks of gestation, the fetal cerebral vascular evaluation might be used to define the best moment of delivery reducing the risk of neurological damage. At this gestational age, in a tertiary center with an acceptable perinatal survival, the main aim of the surveillance is to avoid long term neurological damage. Therefore, increased impedance in the umbilical artery combined with brain vasodilatation might be indications of delivery despite still having diastolic flow in the umbilical artery and/or a normal flow in the ductus venosus. (94, 95)

Fetal Brain Circulation and the risk of neurological damage

Term infants have a different pattern of brain lesion as a consequence of perinatal asphyxia. Although the brain is less vulnerable to white matter damage, when compared with preterm infants, the HIE with involvement of the cerebral cortex is an event that may result in neurodevelopment disabilities, including cerebral palsy,

mental retardation, and learning disabilities. (96, 97)

On the contrary, structural neurological damage in preterm infants is usually manifested as intraventricular hemorrhage (IVH) and/or perivenrticular leucomalacia (PVL). Both manifestations can be present before birth but usually appear within the first 72 h of life and are strongly associated with long-term cognitive and motor disabilities. (98, 99, 100)

Growing evidence shows that the increment of blood flow to the fetal brain might be an early indicator of neurological damage. Earlier studies demonstrated that a reduction in the vascular impedance of the carotid arteries was associated with abnormal fetal blood gases.

Mari et al. studied the MCA-PI in IUGR premature fetuses at 25 to 34 weeks of gestation and found a higher incidence of IVH in fetuses with reduced MCA-PI. (101) Padilla-Gomes et al. studied early-onset IUGR neonates with abnormal Doppler evaluation in the umbilical UA (UA-PI above the 95th percentile) and MCA (MCA-PI below the 5th percentile) and found an increased prevalence of transient periventricular echogenicities, periventricular leucomalacia, and intraventricular hemorrhage than normally grown neonates with normal blood flow in both vessels. (102, 103)

Aside for the PI of the brain arteries, different authors suggest a potential contribution of the waveform velocities in the identification of infants at risk of developing brain damage.

Levene et al. showed that at 24 to 72 h of life, infants with moderate or severe postasphyxial encephalopathy had high cerebral blood flow (CBF) velocities and a significantly lower resistance index, with a positive predictive value of 94% for death

or severe neurological impairment. (103) Ilves et al. reported that at 12 h after birth, the mean blood flow velocity in the ACA or MCA is decreased in asphyxiated infants developing mild or moderate stages of HIE. (104)

Abnormal CPR has been also associated with an increased risk of neurological damage after birth. Jugovic et al. found an increased association between an abnormal CPR and the presence of transient periventricular echodensities and intraventricular hemorrhage.

Maunu et al. reported a significant association of increased CPR and reduced brain volume in neonates born small for gestational age and Roza et al. (2008) showed an altered neurodevelopment in IUGR neonates with abnormal CPR. (105)

The prevalence of cerebral palsy was higher within the group of infants with higher peak blood flow velocities.

4.4 Long Term Neurodevelopment in IUGR Fetuses with Brain Sparing

Clinical studies evaluating long term neurodevelopmental outcome of IUGR fetuses showed differences in the anatomy (CNCO) and function of the fetal brain.

Leitner et al. followed a cohort of IUGR newborns for more than 10 years, documenting a wide spectrum of neurological complications, including visual and acoustic impairments, deficiencies in logical reasoning and problem-solving abilities. (106)

Martin et al. also followed a long-term cohort of IUGR newborns with abnormal Doppler evaluation during gestation and found reduced cognitive skills, abnormal optic nerve morphology, and altered visual capacity. They reported that the degree of weight deviation and Doppler abnormalities correlated with a reduction of the axonal

area of the optic nerve. These children also showed mild altered coordination and poor balance at 7 years of age, probably associated with alterations in the cerebellum and basal ganglia. Children born with IUGR were less successful in scholarly achievements and showed more learning disabilities than those children normally grown at birth. (107)

4.5 Small for Gestational Age Fetuses and Late Intrauterine Growth Restriction

Term SGA fetuses with normal UA Doppler account for nearly 10% of the pregnant population. Although earlier reports suggested that these fetuses might essentially represent constitutionally normal small fetuses, recent evidence demonstrates that this diagnostic category contains a proportion of cases with late-onset IUGR that will present a higher incidence of adverse perinatal outcome, abnormal neurobehavior, and suboptimal neurodevelopment in childhood. (108, 109, 110)

In many of these SGA fetuses presenting an adverse perinatal outcome, longitudinal studies demonstrated that UA impedance remains normal throughout pregnancy, suggesting that the degree of placental insufficiency is not reflected in the UA Doppler but probably in other vascular territories. This was also demonstrated by Hershkovitz et al. who showed that in SGA fetuses at the end of the pregnancy, the middle cerebral artery and the fetal biophysical profile performed better that the UA Doppler in identifying cases at risk for adverse perinatal outcome. (111, 112) Almost half of term SGA fetuses with normal UA Doppler show signs of brain sparing before delivery, which can be identified using different brain Doppler parameters. Each vascular territory has a different sensitivity for early detection of brain redistribution and a different pattern of deterioration.

Fetal brain blood perfusion became affected at around 37weeks in 45% of SGA fetuses, followed by the CPR one week later in 305 cases and finally by the anterior cerebral artery. Finally, MCA-PI decreases below the 5th percentile in less than 15% of cases at around 39 weeks of gestation, indicating a relatively advanced stage of brain blood flow redistribution. (113)

In a retrospective study of 231 SGA fetuses, Severi et al. reported that SGA fetuses with MCA vasodilatation showed an OR of 3.1 for an emergency intrapartum cesarean delivery. Most recently, a prospective clinical study by Cruz- Martinez et al. reported that in 420 SGA cases, the combination of the CPR and MCA Doppler before the onset of labor can be useful in the identification of fetuses at high risk of emergency cesarean delivery for fetal distress and neonatal acidosis. Thus, the possibilities to tolerate the uterine contractions and the chances for a successful vaginal delivery are reduced when the CPR or MCA-PI are reduced. When the CPR is abnormal, but MCA-PI is still within normal range, the risk of emergency cesarean delivery for fetal distress increases to 40% in comparison to 20% in the group with normal CPR. (114)

In the presence of MCA vasodilatation, the risk of fetal distress increases to 60% and the risk of neonatal acidosis to 20%, indicating a reduced fetal tolerance reserve. In addition, cases with MCA vasodilatation have an altered neonatal neurobehavior manifested as an abnormal state of organization and motor skills. Similarly, at 2 years of age, up to 52% of SGA fetuses with abnormal MCA Doppler show an abnormal neurodevelopment scoring lower in communication abilities and problem-solving areas. (106)

SGA fetuses with increased frontal perfusion showed a 30% risk of abnormal

neurobehavior expressed in social interactive organization, state organization, and attention capacity. Although there are recommendations that term SGA fetuses should be continuously monitored as high-risk pregnancies, it is still unclear whether induction of labor is of benefit when signs of brain vasodilatation are present. (107) Growing evidence supports the potential benefits of monitoring the fetal brain Doppler parameters in term SGA fetuses with normal UA Doppler. It might be possible that an abnormal CPR, ACA-PI, FMBV, or MCA-PI can select a group at a higher risk of abnormal neurodevelopment and consider them as late-onset IUGR. The fetal cerebral hemodynamic evaluation might contribute in establishing subgroups of SGA fetuses with progressive risk of fetal distress and in optimizing the optimal time for delivery.

In early and severe IUGR affected fetuses, almost all cases will show signs of brain sparing. The main purpose of the cerebral hemodynamic evaluation is to identify signs of cerebral edema manifested as a late increment in the cerebral vascular resistance. When present, it increases the risk of perinatal mortality and should be considered an ominous sign to deliver fetus. (110, 111, 112, 113)

In severe IUGR fetuses reaching 32 weeks of gestation, a balanced decision must be taken as the neonatal survival rate is at this stage is reasonable. At this moment it might be possible to deliver the fetus in presence of altered umbilical and cerebral circulation but still having normal flow in the ductus venosus.

In late-onset IUGR fetuses, mainly in those ith normal blood flow in the umbilical artery, a fetal cerebral hemodynamic evaluation should be performed. Cases with signs of brain sparing have an increased risk of adverse perinatal out come and abnormal neurodevelopment after birth. Unfortunately, there is still no data available

on the benefits of inducing labor in these cases. A detailed post natal evaluation of the neuroadaptation and neurobehavior might be considered.

Despite encouraging results obtained from the evaluation of the fetal brain hemodynamics, more research is needed as some of the techniques previously described are not yet available in all centers. The brain vascular evaluation is routinely performed but rarely used as an isolated parameter for delivering a compromised fetus.

The contribution of the US techniques here described might help to identify its value in the surveillance of mild and severely affected intrauterine growth restricted fetuses.

Chapter 5

Evaluation of Fetal Cerebral Blood Flow using Power Doppler Ultrasound Angiography in Fetuses affected by Intrauterine Growth Restriction. A pilot study.

5.1 Introduction

The evaluation of fetal brain blood flow can be considered very important because deficits in the perfusion of this territory may lead to inadeguate development of the central nervous system and even jeopardize fetal vitality. (115, 116, 117)

Fetal intrauterine growth restriction (IUGR) associated with placental insufficiency can present well-recognized perinatal and long-term consequences. Some authors demonstrated that neurodevelopment dysfunction in IUGR infants involves general cognitive competence, suggesting dysfunction in the frontal lobe networking limbic system and hippocampus and changes in the morphology of neural structures such as the retinal optical nerve. (116, 117)

The presence of neurological damage originating in different brain areas is associated with an unpaired blood supply. (118)

We can recognise two kind of IUGR fetuses on the basis of the onset of the defect of fetal growth:

- **Early – onset IUGR (before 34 weeks of gestation)** is associated with escalating blood flow resistance in umbilical artery (UA), accompanied by brain sparing followed by deterioration of venous Doppler parameters. Progression is determined by how quickly UA end-diastolic velocity becomes absent or reversed often necessitating preterm delivery.

- **Late – onset IUGR (after 34 weeks of gestation**) is associated with mildly elevated, or even normal, UA Doppler parameters and isolated brain sparing. The deterioration of biophysical parameters is equally subtle and therefore often hard to detect. Cerebro-placental ratio (CPR) decreases with either normal or only minimally elevated UA Doppler indices.

  This is followed by intracerebral redistribution of blood flow towards frontal lobe and basal ganglia. A decreased MCA Doppler index may occur as an isolated finding also without a preeceding increase in UA Doppler Index.

The "brain sparing effect" (blood flow centralization process) can be considered as an adaptive response that preserves brain oxygen supply in the presence of chronic hypoxia. (119, 120)

This process is identified clinically by a reduced Doppler pulsatility index (PI) in the middle cerebral artery (MCA) however, vasodilatation of the MCA might have a poor sensitivity to detect fetuses in the initial stages of increased brain perfusion. longitudinal studies on Doppler evaluation of different brain arteries in the presence of growth restriction suggest that MCA PI is reduced in a later stage than other brain vessels, such as the anterior cerebral artery. (120, 121, 122)

The standard technique used to assess fetal blood flow is usually the bi-dimensional Doppler. In contrast to this conventional method, which analyzes the frequency shift of blood velocity information, power Doppler sonography uses the amplitude component of the signals received to represent the number of moving blood cells. (123)

In fact power Doppler is useful in situations of low-velocity blood flow because it

allows the detection of minimal alterations in blood flow. (124, 125)

Moreover, power Doppler does not show aliasing effect and the colour map is independent of the insonation angle. (126)

The introduction of 3D power Doppler (3D-PD) and the vascularization histogram allowed to quantify the vascularization and blood flow to the placenta and several fetal organs. (127, 128)

The use of 3D-PD is useful in the evaluation of fetal brain vessels because of their small caliber.

5.2 Aim of the study

The aim of the present study is to explore the possible use of 3D Power Doppler Angiography (3D-PDA) using VOCAL^{TM} software (General Electric Healthcare, USA) in the assessment of different cerebral regions in normal and growth restricted fetuses (IUGR). This is a pilot study, that means a small experiment designed to test the method and gather information prior to a larger study.

5.3 Materials and Methods

Between January 2011 and October 2014, 70 singleton pregnancies with intrauterine growth restriction (IUGR) and 183 appropriate for gestational age pregnancies (AGA) as control cases were included. Pregnancies with maternal complications, fetal malformations or chromosomal defects, or conceived after assisted reproduction, were excluded. Gestational age at the enrollment varied between 22 and 38 weeks, based on first trimester ultrasound dating of pregnancy. In all cases the growth potential of each fetus was confirmed after birth.

All ultrasound examinations were performed using General Electric E8 (General Electric Corp., Milkwaukee, WI, USA) with a 5-Mhz transabdominal probe equipped with automatic volume measurements, colour, pulsed and power Doppler options.

IUGR was defined as an ultrasound-estimated fetal weight below the 10th centile for gestational age according to the Hadlock 4 Equation for fetal weight estimation using biparietal diameter, head circumference, abdominal circumference and femur length. (129, 130)

Pulsed wave Doppler flow analysis of the umbilical artery was obtained from a free-floating central section of the cord at an angle close to 0°.

The MCA is sampled at the proximal end of the vessel close to the circle of Willis with a near 0° angle of insonation. each uterine artery can be assessed using the colour Doppler flow to identify the crossing over with the internal iliac artery and vein just before it enters the uterus. Three subsequent blood velocity waveforms for each vessel were analyzed for PI according to Gosling et al. (131)

 For each of these three vessels, an abnormal PI was defined as a deviation from the mean by 20%. The results were checked against previously published reference ranges. (132, 133, 134)

3D-PDA images of the fetal brain were acquired during fetal rest, and using the same presets for each acquisition. The angle of acquisition was set at 35°, the pulsed repetition frequency (PRF) of the power Doppler at 0,9. Power Doppler signals from the fetal brain were recorded in the biparietal plane including landmarks like the thalami, the third ventricle, the cavum septi pellucidi (CSP), the tentorial hiatus, and a symmetrical display of the calvaria (See Figure 1).
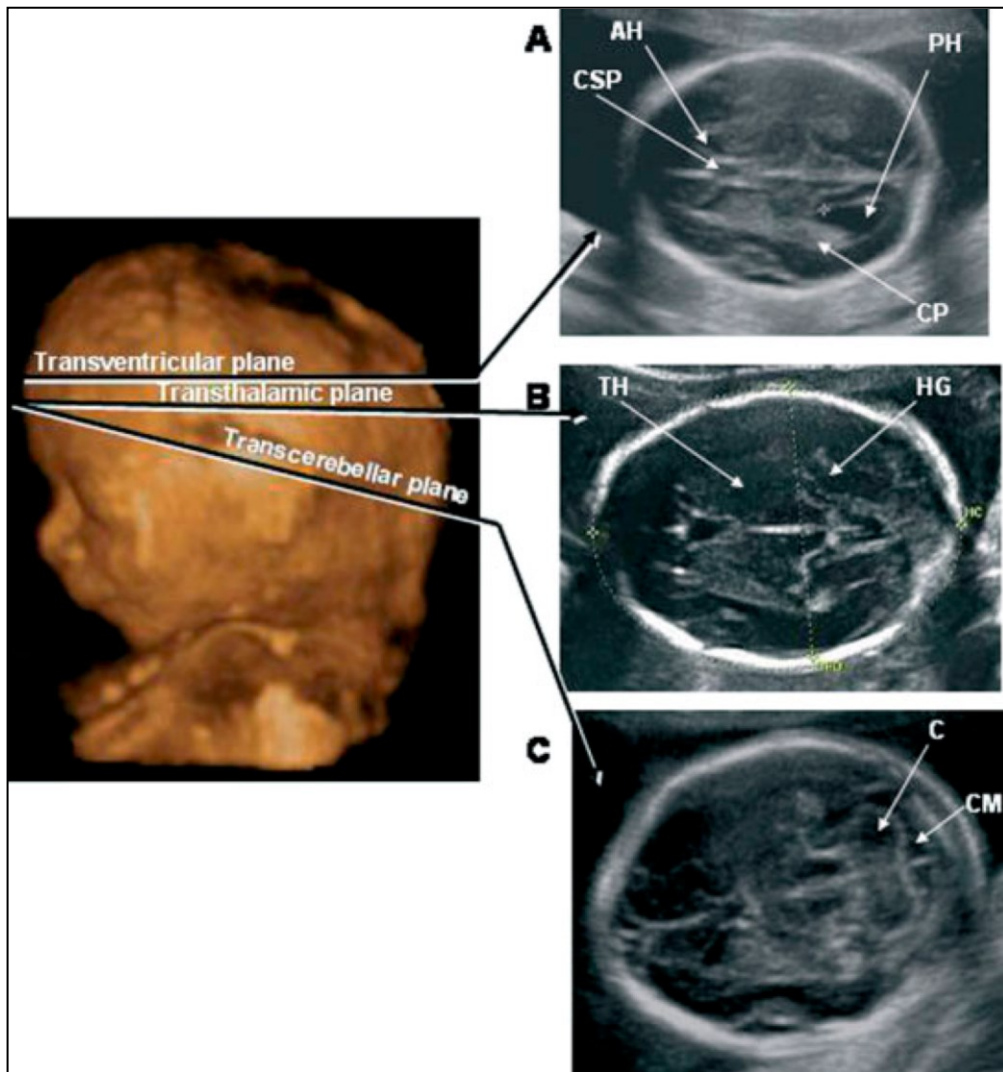
Figure 1

After displaying three simultaneous perpendicular planes on the monitor (axial, sagittal and coronal) the size of the region of interest (ROI) was adapted manually to create the 2 zones of the fetal brain to be analyzed. (Figure 2)
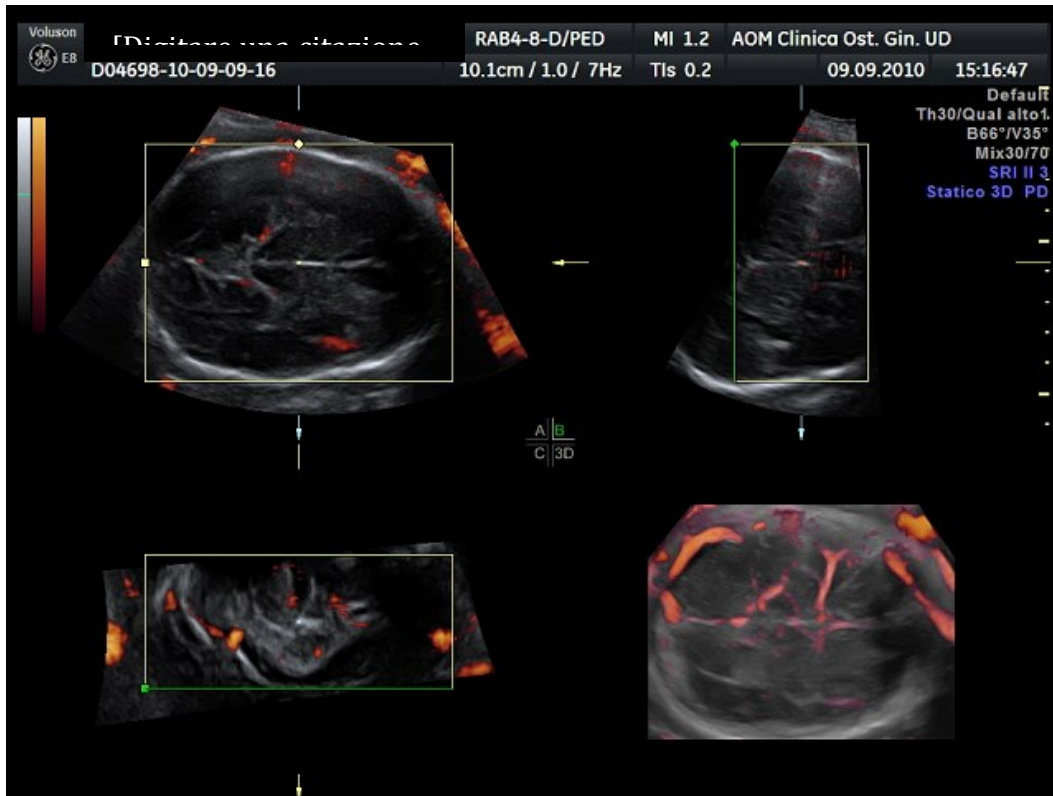
Figure 2 - Three Dimensional Multiplanar View of Fetal Brain

These 2 zones of the fetal brain were defined by using anatomy landmarks to realize a high good reproducibility of this method among different operators. The first zone, named Frontal Zone (Zone 1), was obtained by tracing the contour of the anterior part of the fetal brain up to the perpendicular line crossing the anterior delineation of the CSP (Figure 3, Figure 4). This zone is mainly sprinkled by Anteriore Cerebral Artery (ACA).

The second one, called Temporal Zone (Zone 2), is defined by a rectangle reaching from both temporal bones with the width of CSP included. This zone is sprinkled by Middle Cerebral Artery (MCA) (Figure 3, Figure 5).
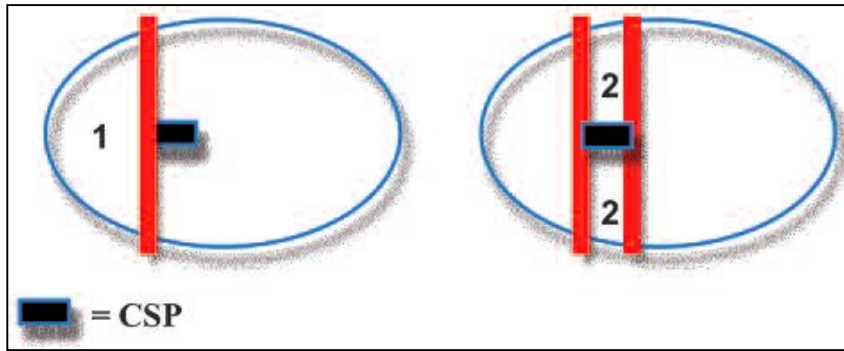
Figure 3 – Definition of 2 Fetal Brain Zones: Frontal Zone (Area 1), Temporal Zone (Area 2)
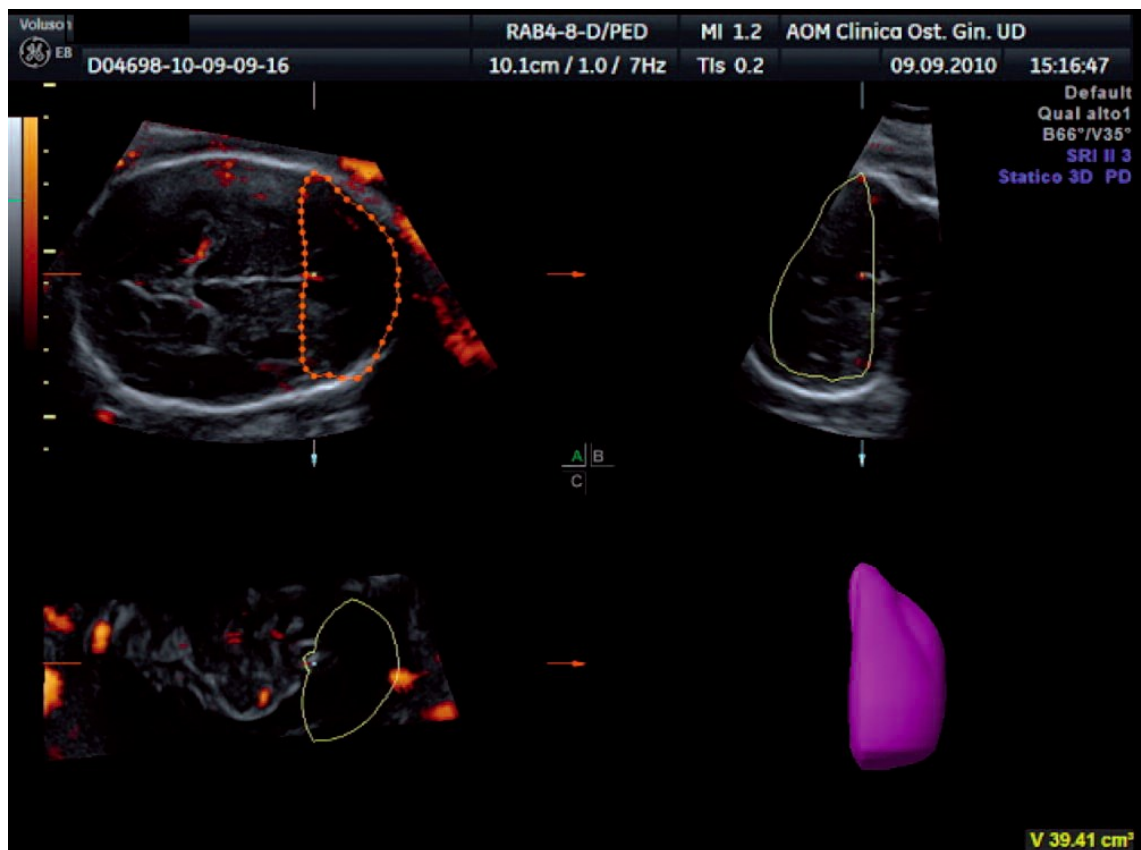
Figure 4 – Frontal Zone of Fetal Brain

The volume of the investigated zones and the blood flow indices were calculated using

VOCAL™ software. A rotation step for each contour plane was selected with a 30°

degree angle chosen arbitrarily.

This procedure of rotating the reference plane was done until a full rotation of 180

degrees was achieved. The fetal brain volumes were calculated after all contours traced (6 steps). Then the Vocal histogram switch was activated for the automatic calculation of the 3D-PDA vascular indices (VI = vascularization index, FI = flow index, VFI = vascularization and flow index). The VI identifies the number of coloured voxels in the ROI, which is an estimate of the number of vessels within that tissue.

The FI is the average colour value of all the colour voxels and represents both the average blood flow intensity. The VFI is the average colour value of all the gray and colour voxels and represents both blood flow and vascularization
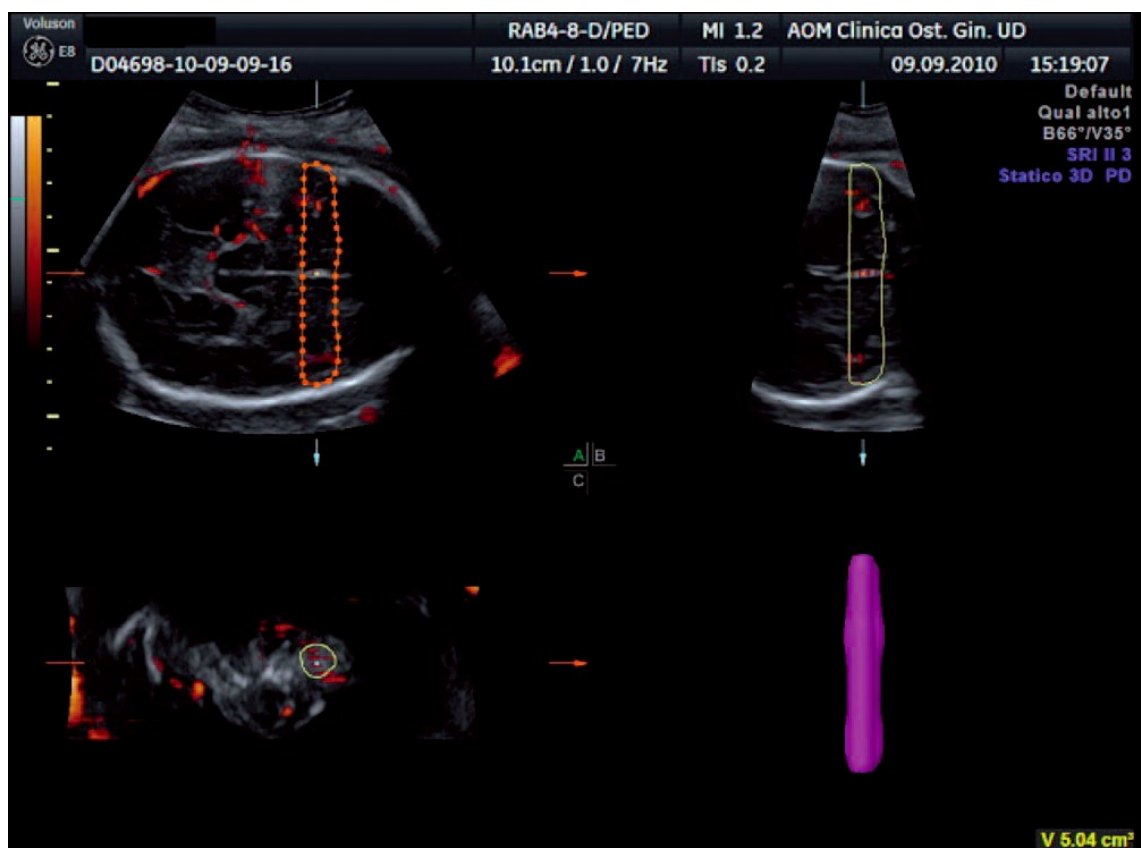
Figure 5 – Temporal Zone of Fetal Brain

For further analysis IUGR fetuses were categorized into one of the following three

groups, based on the Umbilical Artery (UA) Pulsatility Index (PI), Middle Cerebral Artery (MCA) PI and the Ductus venosus (DV) PI:

- **Group 1** (Late onset IUGR): associated with normal UA PI, normal MCA PI and normal DV PI

- **Group 2** (Early onset IUGR):fetuses with abnormal UA PI (> 2 SD), normal MCA PI and normal DV PI

- **Group 3** (Early onset IUGR). fetuses with IUGR have an abnormal UA PI (> 2 SD), an abnormal MCA PI (< 2 SD) and an abnormal DV PI (> 2 SD).

The results of 3D-PDA analysis of zone 1 and zone 2 were correlated with pregnancy outcome parameters at birth, such as gestational age (GA) at delivery, caesarean section (CS) rate, preeclampsia, birthweight, APGAR score, neonatal intensive care unit (NICU) admission, in-utero mortality, neonatal mortality, perinatal mortality. Differences between AGA and growth-restricted foetuses were evaluated using Student's test and differences within different IUGR groups were evaluated by AnOVA test. P < 0,05 was considered significant. The study was approved by the local ethics Committee and written consent was obtained from all participants.

5.4 Results

Table 1 shows the perinatal outcomes and characteristics of the population studied. 70 IUGR fetuses and 183 appropriate-for-gestational age (AGA) fetuses matched by gestational age were evaluated. Considering the IUGR Groups the gestational age (GA) at delivery was similar between all the Groups. Caesarean Section rate was gradually higher in Group 1, Group 2 and in Group 3 compared with the Control Group. 19 cases of IUGR were associated with preeclampsia equally divided among

the 3 different groups. The mean birthweight was lower in Group 1, Group 2 and 3 if compared with Controls. APGAR scores at 1 and 5 min were comparable. The admissions at the Neonatal Intensive Cure Unit (NICU) were more frequent for fetuses affeccted by Early Onset IUGR (Group 2, Group 3) compared with Group 1 (Late Onset Group) and Control Group (AGA). There was one case of intra-uterine fetal death in Group 1.

Table 1 – Perinatal outcomes of the study population (Mean (range or standard deviation) or %)0

	Control Group (AGA n = 183)	Group 1 Late Onset IUGR (n= 34)	Group 2 Early Onset IUGR (n=18)	Group 3 Early Onset IUGR (n=18)
Gestational age (GA) at delivery	39ws+1d (37+1 – 41+3)	35ws+0d (33+1 – 37+2)	34ws+5d (32+5 – 36+3)	34ws+0d (31+5 – 36+2)
Caesaren section rate %	23 % (42/183)	40% (14/34)	48% (8/18)	65% (12/18)
Pre-eclampsia %	2% (4/183)	20%(7/34)	25% (5/18)	40% (7/100)
Birth weight (mean) gr	3342 gr (503)	1916 gr* (99)	2020 gr* (65)	1767 gr* (170)
Apgar Score (1/5 min)	8/9 (1,39/1,92)	7/8 (0,89/0,81)	8/8 (0,57/0,57)	6/9 (1,99/0,48)
NICU admission	2% (3/183)	20% (7/34)	33% (6/18)	33% (6/18)
In utero mortality	0	0,3%(1/34)	0	0
Neonatal mortality	0	0	0	0
Perinatal Mortality	0	0	0	0

* $p < 0,01$ vs Control Group (ANOVA)

Table 2 shows the values of the vascular parameters (VI, FI and VFI) and the volume of the sampled brain in zone 1 for the Control Group and for the IUGR Groups at different hemodynamic stages (Group 1, Group 2 and Group 3).

VI and VFI values were significantly increased in Late Onset IUGR fetuses (Group 1) compared to Control Group (AGA).

Table 2 – Three dimensional Power Doppler Angiography parameters values in Zone 1 in the Control Group and Foetuses with Intrauterine Growth Restrictions at different hemodynamic stages (Group 1, Group 2 and Group 3)

	Vascularity Index (V.I.)	Flow Index (F.I.)	Vascularity Flow Index	Volume (cm^3)
Control Group (AGA n = 183)	2,27 (0,3)	31,96 (7)	0,73 (0,3)	32,92 (6,27)
Group 1 Late Onset IUGR (n= 34)	5,53* (2,1)	24,12 (5,8)	1,35* (0,6)	17,25 (4,6)
Group 2 Early Onset IUGR (n=18)	1,48 (0,25)	26,6 (5,9)	0,55 (0,025)	20,87 (5,6)
Group 3 Early Onset IUGR (n=18)	2,16 (0,2=	31,21 (6,9)	0,75 (0,05)	29,0 (6,1)

Mean value and standard deviation of 3DPDA in each Group. Group 1, normal umbilical artery (UA) pulsatily index (PI) and normal middle cerebral artery (MCA) PI ;Group 2 , abnormal umbilical artery (UA) pulsatily index (PI) (mean > 2 SD) and normal middle cerebral artery (MCA) PI ; Group 3 abnormal umbilical artery (UA) pulsatily index (PI) (mean >2 SD) and abnormal middle cerebral artery (MCA) PI (PI < 2 SD) and pathological ductus venous (DV) PI (mean>2 SD). AGA, appropriate for gestational age.* $P<0,05$ vs Controls (Student's t-test) and $p<0,05$ vs Group 2 and Group 3 (ANOVA).

Table 3 shows the results of the VI, FI and VFI and the volume of the sampled brain in zone 2 in the Control Group and in the fetuses with IUGR at different hemodynamic stages.

VI and VFI values were significantly decreased in fetuses with Late Onset IUGR (normal values of fetal arterial and venous Doppler (Group 1) compared to Control Group.

The VFI both in the Group 2 and 3 (Early Onset IUGR) were very significantly increased compared to Control Group. Besides, the volume of the sampled brain (zone 2) is significantly increased in the fetuses with an abnormal UA PI and a normal MCA PI.

Table 3 – Three dimensional Power Doppler Angiography vascular parameters values in Zone 2 in the Control Group and Foetuses with Intrauterine Growth Restrictions at different hemodynamic stages (Group 1, Group 2 and Group 3)

	Vascularity Index (V.I.)	Flow Index (F.I.)	Vascularity Flow Index	Volume (cm^3)
Control Group (AGA n = 183)	3,38 (0,6)	27,67 (5,8)	1,15 (0,3)	5,13 (1,2)
Group 1 Late Onset IUGR (n= 34)	0,95* (0,3)	26,56 (7,6)	0,21* (0,1)	2,81 (0,7)
Group 2 Early Onset IUGR (n=18)	4,95 (1,2)	30,29 (7,7)	2,10* (0,2)	7,10* (2,3)
Group 3 Early Onset IUGR (n=18)	5,17 (1,2)	34,09 (6,3)	3,5** (0,2)	5,21 (1,5)

Mean value and standard deviation of 3DPDA in each Group. Group 1, normal umbilical artery (UA) pulsatily index (PI) and normal middle cerebral artery (MCA) PI ;Group 2 , abnormal umbilical artery (UA) pulsatily index (PI) (mean > 2 SD) and normal middle cerebral artery (MCA) PI ; Group 3 abnormal umbilical artery (UA) pulsatily index (PI) (mean >2 SD) and abnormal middle cerebral artery (MCA) PI (PI < 2 SD) and pathological ductus venous (DV) PI (mean>2 SD). AGA, appropriate for gestational age.
* $P<0,05$ vs Controls (Student's t-test) and $p<0,05$ vs Group 2 and Group 3 (ANOVA)
** $P<0,05$ vs Controls (Student's t-test) and $p<0,05$ vs Group 1 and Group 2 (ANOVA)

5.5 Discussion

In Late Onset IUGR fetuses (Group 1), presenting normal Bidimensional Doppler flow indices of umbilical and middle cerebral arteries, Vascularity Index (VI) and Vascular Flow Index (VFI) of the frontal zone of the fetal brain resulted increased demonstrating the *"frontal brain sparing effect"* . On the other hand, these vascular parameters were decreased in the temporal zone suggesting a vascular redistribution during brain sparing effect according to a regional increase in bloody supply to the frontal region sprinkled mainly by the anterior cerebral artery. This shift may indicate that general cognitive functions, such as impulse control, language, memory, problem solving and socialization may be preferentially preserved suggesting a hierarchical order in the protection of the brain functions. (135)

Besides our preliminary findings are in line with recent studies in growth-restricted

fetuses, suggesting that the anterior cerebral artery shows Doppler signs of vasodilatation before these are observed in the MCA. (121, 122)

The data on the Vascular Flow Index of the Temporal Zone, sprinkled mainly by the Middle Cerebral Artery, in both Groups of Early Onset IUGR, with and without abnormal bidimensional Middle Cerebral Artery findings (Group 2 and 3), revealed a preferential increment in bloody supply to the temporal region.

Most current clinical protocols for fetal growth restriction are based on the assumptions that the onset of a brain-sparing effect is indicated by a reduced Middle Cerebral Artery Pulsatility Index (MCA PI), representing a protective hemodynamic response in the entire fetal brain.

The results obtained by power Doppler Angiography (3D-PDA) show a different pattern of vascular blood distribution in the brain of IUGR fetuses in relation to the bidimensional Doppler findings.

MCA vasodilatation (MCA PI reduction) may do not represent a protective response but rather the starting point after which the protection of the frontal area begins to decline.

The *"real brainsparing effect"* seems to be marked by hemodynamic changes in the anterior cerebral artery (ACA) and consequently in its districts. If confirmed, these findings might have important implications, especially since Doppler findings may be subtle and accurate identification of growth restriction arising in the third trimester still provides a challenge.

The clinical significance of the observations reported in the present study remains to be established by larger prospective studies with long term postnatal neurological follow-up.

According to these results, 3D sonography and power Doppler angiography can be considered as new techniques offering to study additional vascular parameters of the fetal brain allowing the evaluation of non invasive "brain sparing markers" in IUGR fetuses.

Three Dimensional Power Doppler Angiography (3D PDA) could be considered as an important tool to evaluate fetal well-being for fetus affected by Late Onset IUGR, adding more informations compared with traditionl parameters obtained using only bidimensional Doppler.

Three Dimensional Power Doppler Angiography (3D PDA) could be considered as a new method to detect high risk pregancies and it should be included in the protocols to define the timing of the delivery.

Furthermore, construction of reference charts and an intra- inter- observer variability study of vascular indices of fetal brain circulation obtained in 3D-PDA mode in normal pregnancies will be planned.

The clinical significance of the observations reported in the present study remains to be established by larger prospective studies with long term post - natal neurological follow-up.

References

1. Timor-Tritsch IE, Monteagudo A. Transvaginal fetal neurosonography: standardization of the planes and sections by anatomic landmarks. Ultrasound Obstet Gynecol 1996; 8: 42–47.

2. Malinger G, Katz A, Zakut H. Transvaginal fetal neurosonography. Supratentorial structures. Isr J Obstet Gynecol 1993; 4:1–5.

3. Pilu G, Segata M, Ghi T, Carletti A, Perolo A, Santini D, Bonasoni P, Tani G, Rizzo N. Diagnosis of midline anomalies of the fetal brain with the three-dimensional median view. Ultrasound Obstet Gynecol 2006; 27: 522–529.

4. Monteagudo A, Timor-Tritsch IE, Mayberry P. Three-dimensional transvaginal neurosonography of the fetal brain:'navigating' in the volume scan. Ultrasound Obstet Gynecol 2000; 16: 307–313.

5. Van den Wijngaard JA, Groenenberg IA, Wladimiroff JW, Hop WC. Cerebral Doppler ultrasound of the human fetus. Br J Obstet Gynaecol 1989; 96: 845–849.

6. Filly RA, Cardoza JD, Goldstein RB, Barkovich AJ. Detection of fetal central nervous system anomalies: a practical level of effort for a routine sonogram. Radiology 1989; 172: 403–408.

7. 18. Falco P, Gabrielli S, Visentin A, Perolo A, Pilu G, Bovicelli L. Transabdominal sonography of the cavumseptumpellucidumin normal fetuses in the second and third trimesters of pregnancy.
Ultrasound Obstet Gynecol 2000; 16: 549–553.

8. Malinger G, Lev D, Kidron D, Heredia F, Hershkovitz R, Lerman-Sagie T. Differential diagnosis in fetuses with absent septum pellucidum. Ultrasound Obstet Gynecol 2005; 25: 42–49.

9. Pilu G, Reece EA, Goldstein I, Hobbins JC, Bovicelli L. Sonographic evaluation of the normal developmental anatomy of the fetal cerebral ventricles: II. The atria. Obstet Gynecol 1989; 73: 250–256.

10. Cardoza JD, Filly RA, Podrasky AE. The dangling choroid plexus: a sonographic observation of value in excluding ventriculomegaly. AJR Am J Roentgenol 1988; 151: 767–770.

11. Cardoza JD, Goldstein RB, Filly RA. Exclusion of fetal ventriculomegaly with a single measurement: the width of the lateral ventricular atrium. Radiology 1988; 169:

711–714.

12. Mahony BS, Nyberg DA, Hirsch JH, Petty CN, Hendricks SK, Mack LA. Mild idiopathic lateral cerebral ventricular dilatation in utero: sonographic evaluation. Radiology 1988; 169: 715–721.

13. Shepard M, Filly RA. A standardized plane for biparietal diameter measurement. J Ultrasound Med 1982; 1: 145–150.

14. Snijders RJ, Nicolaides KH. Fetal biometry at 14–40 weeks' gestation. Ultrasound Obstet Gynecol 1994; 4: 34–48.

15. Pilu G, Falco P, Gabrielli S, Perolo A, Sandri F, Bovicelli L. The clinical significance of fetal isolated cerebral borderline ventriculomegaly: report of 31 cases and review of the literature.
Ultrasound Obstet Gynecol 1999; 14: 320–326.

16. Kelly EN, Allen VM, Seaward G, Windrim R, Ryan G. Mild ventriculomegaly in the fetus, natural history, associated findings and outcome of isolated mild ventriculomegaly: a literature review. Prenat Diagn 2001; 21: 697–700.

17. Wax JR, Bookman L, Cartin A, Pinette MG, Blackstone J. Mild fetal cerebral ventriculomegaly: diagnosis, clinical associations, and outcomes. Obstet Gynecol Surv 2003; 58: 407–414.

18. Laskin MD, Kingdom J, Toi A, Chitayat D, Ohlsson A. Perinatal and neurodevelopmental outcome with isolated fetal ventriculomegaly: a systematic review. J Matern Fetal Neonatal
Med 2005; 18: 289–298.

19. Achiron R, Schimmel M, Achiron A, Mashiach S. Fetal mild idiopathic lateral ventriculomegaly: is there a correlation with fetal trisomy? Ultrasound Obstet Gynecol 1993; 3: 89–92.

20. Gaglioti P, Danelon D, Bontempo S, Mombro M, Cardaropoli S, Todros T. Fetal cerebral ventriculomegaly: outcome in 176 cases. Ultrasound Obstet Gynecol 2005; 25: 372–377.

21. Heiserman J, Filly RA, Goldstein RB. Effect of measurement errors on sonographic evaluation of ventriculomegaly. J Ultrasound Med 1991; 10: 121–124.

22. Sonographic Guidelines ISUOG - Sonographic examination of the fetal central nervous system:
guidelines for performing the 'basic examination' and the 'fetal neurosonogram'. Ultrasound Obstet Gynecol 2007; 29: 109–116.

23. Mahony BS, Callen PW, Filly RA, Hoddick WK. The fetal cisterna magna. Radiology 1984; 153: 773–776.

24. Malinger G, Katz A, Zakut H. Transvaginal fetal neurosonography. Supratentorial structures. Isr J Obstet Gynecol 1993; 4:1–5.

25. Monteagudo A, Timor-Tritsch IE. Development of fetal gyri, sulci and fissures: a transvaginal sonographic study. Ultrasound Obstet Gynecol 1997; 9: 222–228.

26. Toi A, Lister WS, Fong KW. How early are fetal cerebral sulci visible at prenatal ultrasound and what is the normal pattern of early fetal sulcal development? Ultrasound Obstet Gynecol 2004; 24: 706–715.

27. Droulle P, Gaillet J, Schweitzer M. [Maturation of the fetal brain. Echoanatomy: normal development, limits and value of pathology]. J Gynecol Obstet Biol Reprod (Paris) 1984; 13:
228–236.

28. Cohen-Sacher B, Lerman-Sagie T, Lev D, Malinger G. Sonographic developmental milestones of the fetal cerebral cortex: a longitudinal study. Ultrasound Obstet Gynecol 2006; 27: 494–502.

29. Crane JP, LeFevre ML, Winborn RC, Evans JK, Ewigman BG, Bain RP, Frigoletto FD, McNellis D. A randomized trial of prenatal ultrasonographic screening: impact on the detection,
management, and outcome of anomalous fetuses. The RADIUS Study Group. Am J Obstet Gynecol 1994; 171:392–399.

30. Ewigman BG, Crane JP, Frigoletto FD, LeFevre ML, Bain RP, McNellis D. Effect of prenatal ultrasound screening on perinatal outcome. RADIUS Study Group. N Engl J Med 1993; 329:
821–827.

31. Bennett GL, Bromley B, Benacerraf BR. Agenesis of the corpus callosum: prenatal detection usually is not possible before 22 weeks of gestation. Radiology 1996; 199: 447–450.

32. Scheel P., Ruge C., Petruch U.R.: Color duplex measurement of cerebral blood flow volume in healthy adults. Stroke 2000; 31: 147-150.

33. Mai J.K., Assheuer J., Paxinos G.: Atlas of the Human Brain. Academic Press, San Diego, 1997.

34. Kaplan H.A., Ford D.H.: "The Brain Vascular System", Elsevier, Amsterdam, 1966.

35. Morris P.: "Practical Neuroangiography", Williams & Wilkins, Baltimore, 1997.

36. Willis T.: "Cerebri Anatome". Martin & Allestry, London.

37. Riggs H E., Rupp C: "Variation in the form of the circle of Willis", Arch Neurol 1963; 8, 24-30.

38. Hoksbergen AW, Fulesdi B: "Collateral configuration of the circle of Willis: Transcranial color-coded duplex ultrasonography and comparision with postmortem anatomy". Stroke 2000; 31, 1346-51.

39. Van Der Zwan A, Hillen B, Tulleken CA: " Variability of the territories of the major cerebral arteries". J. Neurosurg, 1992; 77; 927 – 940.

40. Goldberg BB, Merton DA, Deane CR: "An Atlas of Ultrasound Color Flow Imaging". London: Martin Dunitz, 1997.

41. Van Der Zwan A, Hillen B, Tulleken CA: " Variability of the territories of the major cerebral arteries". J. Neurosurg, 1992; 77; 927 – 940.

42. Scremin OU: "Cerebral Vascular System". The Human Nervous System, Elsevier, 2004.

43. Clarke E., O' Malley C.D.: "The Human Brain and Spinal Cord - A Historical Essay Illustrated by Writings from Antiquity to the Twentieth Century", University of California Press, Berkeley, Los Angeles.

44. Evans DH, Mc Dicken WN, Skidmore R: Doppler Ultrasound: "Phisics, Instrumentation and Clinical Application". Chicester: Wiley, 1989.

45. Powis RL, Schwarz RD: "Practical Doppler Ultrasound for the Clinician". Williams and Wilkins, 1991.

46. Goldberg BB, Merton DA, Deane CR: "An Atlas of Ultrasound Color Flow Imaging". London: Martin Dunitz, 1997.

47. Gill RW: "Measurement of blood flow by ultrasound: accuracy and source of error". Ultrasound Med Biol 1985; 7; 625 – 642.
48. Nicolaides KH, Rizzo G, Hecher K: "Placental and fetal Doppler". New York: The Parthenon Publishing Group, 2000.

49. Schulman H, Fleischer A, Farmakides G: "Development of uterine artery compliance in pregnancy as detected by Doppler ultrasound". Am J Obstet Gynecol, 1986; 155; 1031 – 6.

50. Arduini D, Rizzo G, Boccolini MR: "Functional assessment of utero-placental and fetal circulation by means of Color Doppler ultrasonography". J Ultrasound Med, 1990; 9: 249-53.

51. Maulik D: "Basic principles of Doppler ultrasound as applied in obstetrics". Clin Obstet Gnecol, 1989; 32: 628-44.

52. Kirkinen P, Muller R, Huch R: "Blood flow velocity waveforms in human fetal intracranial arteries." Obstet Gynecol, 1987; 70: 617-21.

53.Battaglia FC, Lubchenko LO. A practical classification of newborn infants by weight and gestational age. J Pediatr 1967; 71:159-163.

54.American College of Obstetricians and Gynecologists. Intrauterine Growth Restriction; ACOG practice bulletin no.12. Washington, DC: ACPG; 2000.

55. Baschat AA. Arterial and venous Doppler in the diagnosis and management of early onset fetal growth restriction. Early Hum Dev 2005; 81: 877-87.

56. Gardosi j, Francis A. Adverse pregnancy outcome and association with small for gestational age birthweight by customized and population-based percentiles. Am J Obstet Gynecol 2009; 201: 28.

57. Baschat AA. Pathophysiology of fetal growth restriction: implications fordiagnosis and surveillance. Obstet Gynecol Surv , 59(8):617_627, Aug 2004.

58. Trudinger BJ. Doppler ultrasonography and fetal well being. Reece EA, Hobbins JC, Mahoney M. Medicine of the fetus and mother. Philadelphia, PA: JB Lipincott Co; 1992.

59. Fisk NM, MacLachian N, Ellis C. Absent end-diastolic flow in first trimester umbilical artery. Lancet 1988; 2: 1256-7.

60. Trudinger BJ, Stevens D, Connely A. Umbilical artery flow velocity waveforms and placental resistance: the effect of embolizations of the umbilical circulation. Am I Obstet Gynecol 1987; 157: 1443-8.

61. Dubiel M, Gunnarsson GO. Blood redistribution in the fetal brain during chronic hypoxia. Ultrasound Obstet Gynecol 2002; 20: 117-21.

62. McIntire DD, Bloom SL, Casey BM. Birth weight in relation to morbidity and mortality among newborn infants. N Engl J Med 1999; 340: 1234-8.

63. Baschat AA, Gembruch U. The Cerebroplacental Doppler ratio revisited. Ultrasound Obstet Gynecol 2003; 21: 124-7.

64. Bahado-Singh RO, Kovanci E. The Doppler Cerebroplacental ratio and Perinatal Outcome in Intrauterine growth restriction. Am J Obstet Gynecol 1999; 180: 750-6.

65.Odibo AO, Riddick C. Cerebroplacental Doppler ratio and adverse perinatal outcomes in intrauterine growth restriction: evaluation of the impact of using gestational age-specific reference values. J Ultrasound Med 2005; 24: 1223-8.

66. Edelstone DI, Rudolph AM: "Preferential streaming of ductus venosus blood flows in fetal lambs in utero". Circ Res; 1978; 42: 426-33.

67. Van den Wijngaard JA, Groenenberg IA. Cerebral Doppler Ultrasound of the Human fetus. Br J Obstet Gynecol 1989; 96: 845-9.

68. Vyas S, Nicolaides KH. Middle crebral artery flow velocity waveforms in fetal hypoxaemia. Br J Obstet Gynecol 1990; 97: 797-803.

69. Vyas S, Nicolaides KH, Bower S: "Middle cerebral artery flow velocity waveforms in fetal hypoxaemia". Br J Obstet Gynecol, 1990; 97: 797-803.

70. Arbeille PH, Tranquart F, Berson M. Visualization of the fetal Circle of Willis and intra-cerebral arteries by color-coded Doppler. Eur J Obstet Gynecol Reprod Biol 1989; 32: 195-8.

71. Figueroa-Diesel H. Hernandez-Andrade E. Doppler changes in the main fetal brain arteries at different stages of hemodinamic adaptation in severe intrauterine growth restriction. Ultrasound Obstet Gynecol 2007; 30: 297-302.

72. Benavides-Serralde A, Scheier M, Cruz-Martinez R. Changes in Central and Peripheral Circulation in Intrauterine Growth-Restricted Fetuses at different stages of Umbilical Artery Flow deterioration: New Fetal Cardiac and Brain Parameters. Gynecol Obstet Invest 2011; 71: 274-80.

73. Hernandez-Andrade E, Figueroa-Diesel H, Jansson T. Changes in regional fetal cerebral blood flow perfusion in relation to hemodynamic deterioration in severely growth-restricted fetuses. Ultrasound Obstet Gynecol 2008; 32: 71-6.

74. Cruz-Martinez R, Figueras F, Oros D. Cerebral blood perfusion and neurobehavioral performance in full-term small-for-gestational- age fetuses. Am J Obstet Gynecol 2009; 201: e1-e7.

75. Cruz-Martinez R, Figueras F, Hernandez-Andrade E. Longitudinal brain perfusion changes in near-term small-for-gestational-age fetuses as measured by spectral Doppler indices or by fractional moving blood volume. Am J Obstet Gynecol 2010; 203 (42): e1-e6.

76. Rubin JM, Bude RO, Fowlkes JB Normalizing fractional moving blood volume estimates with Power Doppler US: defining a stable intravascular point with the cumulative power distribution function. Radiology 1997; 205: 757-65.

77. Hernandez-Andrade E, Jansson T, Ley D Validation of fractional moving blood volume measurement with Power Doppler Ultrasound in an experimental sheep model. Ultrasound Obstet Gynecol 2004; 23: 363-8.

78. Cruz-Martinez R, Figueras F, Oros D. Normal reference ranges of fetal regional cerebral blood perfusion as measured by fractional moving blood volume. Ultrasound Obstet Gynecol 2011; 37: 196-201.

79. Hernandez-Andrade E, Figueroa-Diesel H, Jansson T. Changes in regional fetal cerebral blood flow perfusion in relation to hemodynamic deterioration in severely growth-restricted fetuses. Ultrasound Obstet Gynecol 2008; 32: 71-6.

80. Cruz-Martinez R, Figueras F, Oros D. Cerebral blood perfusion and neurobehavioral performance in full-term small-for-gestational- age fetuses. Am J Obstet Gynecol 2009; 201: e1-e7.

81. Dubiel M, Hammid A, Breborowicz A. Flow index evaluation of 3-D volume flow images: an in vivo and in vitro study. Ultrasound Med Biol 2006; 32: 665-71.

82. Bartha JL, Moya EM, Hervìas-Vivancos B Three Dimensional power Doppler analysis of cerebral circulation in normal and growth-restricted fetuses. J Cereb Blood Flow Metab 2009; 29: 1609-18.

83. Benavides-Serralde A, Hernàndez-Andrade E. Three-dimensional sonographic calculation of the volume of intracranial structures in growth-restricted and appropriate-for-gestational-age fetuses. Ultrasound Obstet Gynecol 1993; 5: 195-203.

84. Rossi A, Romanello I, Forzano L. Evaluation of fetal cerebral blood flow perfusion using Power Doppler ultrasound angiography (3D-PDA) in growth restricted fetuses. F. V & V. in ObGyn. 2011, 3 (3): 175-180.

85. Rossi A, Romanello I, Forzano L Assessment of Fetal Brain Vascularization using Three-Dimensional Power Doppler Ultrasound Angiography in Pregnancies affected by Late-Onset Fetal Growth Restrisction. Global Journal of Medical Research. Vol XIV, Issue 1, Year 2014.

86. Maunu J, Ekholm E, Parkkola R. Antenatal Doppler Measurements and Early Brain Injury in Very Low Birth Weight Infants. J Pediatr 2007; 150: 51-6.

87. Roza SJ, Strrgers EA, Verburg BO. What is spared by fetal brainsparing? Fetal circulatory redistribution and behavioral problems in the general population. Am J Epidemiol 2008; 168: 1145-52.

88. Leitner Y, Fattal-Valevski A, Geva R. Neurodevelopmental out come of children with intrauterine growth retardation: a longitudinal, 10 year-prospective study. J Child Neurol 2007; 22:580-7.

89. Cruz-Martinez R, Figueras F, Hernandez-Andrade E. Fetal brain Doppler to predict cesarean delivery for nonreassuring fetal status in term small-for-gestational-age fetuses. Obstet Gynecol 2011; 117: 618-26.

90. Konie JC, Bell SC, Taylor DJ. Abnormal Doppler velocimetry and blood flow volume in the middle cerebral artery in very severe intrauterine growth restriction: is the occurrence of reversal of compensatory flow too late? BJOG 2001; 108: 973-9.

91. Hernandez-Andrade E, Crispi F, Benavides-Serralde A. Contribution of the myocardial performance index and aortic isthmus blood flow index to predicting mortality in preterm growth-restricted fetuses. Ultrasound Obstet Gynecol 2009; 34: 430-6.

92. Figueras F, Eixarch E, Meler E. Small-for-gestational-age fetuses with normal umbilical artery Doppler have suboptimal perinatal and neurodevelopmental out come. Eur J Obstet Gynecol Reprod Biol, 2008; 136: 34-8.

93. Spinillo A, Montanari L, Roccio M. Prognostic significance of the interaction between abnormal umbilical and middle cerebral artery restriction. Acta Obstet Gynecol Scand 2009; 88: 159-66.

94. Mari G, Abuhamad AZ, Keller M. Is the fetal brain-sparing effect a risk factor for the development of intraventricular hemorrhage in the preterm infant? Ultrasound Obstet Gynecol 1996; 8: 329-32.

95. Padilla-Gomes NF, Enriquez G. Prevalence of neonatal ultrasound brain lesions in premature infants with and without intrauterine growth restriction. Acta Paediatr 2007; 96: 1582-7.

96. Leijser LM, Vein AA, Liauw L. Prediction of short-term neurological out come in full-term neonates with hypoxic-ischaemic encephalopathy based on combined use of electroencephalogram and neuro-imaging. Neuropediatrics 2007; 38: 219-27.

97. Gaddlin PO, Finnstrom O. A fifteen-year follow-up of neurological conditions in VLBW children without overt disability: relation to gender, neonatal risk factors and end stage MRI findings. Early Hum Dev 2008; 84: 343-9.

98. Mari G, Abuhamad AZ, Keller M. Is the fetal brain-sparing effect a risk factor for the development of intraventricular hemorrhage in the preterm infant? Ultrasound Obstet Gynecol 1996; 8: 329-32.

99. Padilla-Gomes NF, Enriquez G. Prevalence of neonatal ultrasound brain lesions in premature infants with and without intrauterine growth restriction. Acta Paediatr 2007; 96: 1582-7.

100. Levene MI, Fenton AC, Evans DH. Severe birth asphysia and abnormal cerebral blood-flow velocity. Dev Med Child Neurol 1989; 31: 427-34.

101. Mari G, Abuhamad AZ, Keller M. Is the fetal brain-sparing effect a risk factor for the development of intraventricular hemorrhage in the preterm infant? Ultrasound Obstet Gynecol 1996; 8: 329-32.

102. Padilla-Gomes NF, Enriquez G. Prevalence of neonatal ultrasound brain lesions in premature infants with and without intrauterine growth restriction. Acta Paediatr 2007; 96: 1582-7.

103. Levene MI, Fenton AC, Evans DH. Severe birth asphysia and abnormal cerebral blood-flow velocity. Dev Med Child Neurol 1989; 31: 427-34.

104. Ilves P, Talvik R. Changes in Doppler ultrasonography in asphyxiated term infants with hypoxic-ischaemic encephalopathy. Acta Paediatr 1998; 87: 680-4.

105. Jugovic D, Tumbri J. New Doppler index for prediction of perinatal brain damage in growth-restricted and hypoxic fetises. Ultrasound Obstet Gynecol 2007; 30: 303-11.

106. Leijser LM, Vein AA, Liauw L. Prediction of short-term neurological out come in full-term neonates with hypoxic-ischaemic encephalopathy based on combined use of electroencephalogram and neuro-imaging. Neuropediatrics 2007; 38: 219-27.

107. Martin L, Ley D, Marshal K. A Visual function in young adults following intrauterine growth retatrdation. J Pediatr Ophthalmol Strabismus 2004; 41: 212-8.

108. Figueras F, Figueras J, Meler E. Customised birthweight standards accurately predict perinatal morbidity. Arch Dis Child Fetal Neonatal Ed 2007; 92: F277-80.

109. Figueras F, Oros D, Cruz-Martinez R. Neurobehavior in term, small-for-gestational age infants with normal placental function. Pediatrics 2009; 124: e934-e41.

110. Mc Cowan LM, Pryor J, Harding JE. Perinatal predictors of neurodevelopmental out come in samll-for-gestational- age children 18 months of age. J Obstet Gynecol 2002; 186: 1069-75.

111. Oros D, Figueras F, Cruz-Martinez R. Middle versus anterior cerebral artery Doppler for the prediction of perinatal out come and neonatal neurobehavior in term small-for-gestational age fetuses with normal umbilical artery Doppler. Ultrasound Obstet Gynecol 2010; 35: 456-61.

112. Hershkovitz R, Kingdom JC, Geary M. Fetal cerebral blood flow redistribution in late gestation: identification of compromise in small fetuses with normal umbilical artery Doppler Ultrasound. Obstet Gynecol 1992; 15: 209-12.

113. Cruz-Martinez R, Figueras F, Hernandez-Andrade E. Longitudinal brain perfusion changes in near-term small for gestational age fetuses as measured by spectral Doppler indices or by fractional moving blood volume. Am J Obstet Gynecol 2010; 203 (42): e1-e6.

114. Ilves P, Talvik R. Changes in Doppler ultrasonography in asphyxiated term infants with hypoxic-ischaemic encephalopathy. Acta Paediatr 1998; 87: 680-4.

115. Fouron JC, Gosselin J, Raboisson MJ. The relationship between an aortic isthmus blood flow velocity index and the postnatal neurodevelopmental status of fetuses with placental circulatory insufficiency. Am J Obstet Gynecol. 2005;192:497-503.

116. Geva R, Eshel R, leitner y. neuropsycological out come in children with intrauterine growth restriction: a 9-year prospective study. Pediatrics. 2006;118:91-100.

117. Geva R, eshel R, leitner y. Memory functions of children bornwith asymmetric intrauterine growth restriction. brain Res. 2006;1117:186-194.

118. Scherjon S, briet J, Oosting h, Kok J. The discrepancy between maturation of visual-evoked potentials and cognitive out come at five years in very pretermi infants with and without hemodynamic signs of fetal brain-sparing. Pediatrics. 2000;105: 385-391.

119. Marsal K. Intrauterine growth restriction. Curr Opin Obstet Gynecol. 2002;14:127-135.

120. Baschat AA, Gembruch U, Reiss I. Relationship between arterial and venous Doppler and perinatal out come in fetal growth restriction. Ultrasound Obstet Gynecol. 2000;16:407-413.

121. Dubiel M, Gunnarsson GO, Gundmusson S. blood redistribution in the fetal brain during chronic hypoxia. Ultraound Obstet Gynecol. 2002; 20:117-121.

122. Figueroa-Diesel h, hernandez-Andrade e, Acosta-Rojas R. Doppler changes in the main fetal brain arteries at different stages hemodynamic adaption in severe intrauterine growth restriction. Ultrasound Obstet Gynecol. 2007; 30:297-302.

123. Pairleitner h, Steiner h, hasenoehrl G, Staudach A. Threedimensional power Doppler sonography: Imaging and quantifying blood flow and vascularization. Ultrasound Obstet Gynecol. 1999;14:139-143.

124. Rubin JM, Adler RS, Fowlkes Jb, Spratt S, Pallister Je, Chen JF, Carson Pl. Fractional moving blood volume: estimation with power Doppler US. Radiology. 1995;197:183-190.

125. Rubin JM, bude RO, Carson Pl, bree Rl, Adler RS. Power Doppler US: A potentially useful alternative to mean frequency- based color Doppler. Radiology. 1994;190:853-856.

126. Yu Ch, Chang Ch, Ko hC, Chen WC, Chang FM. Assessment of placental fractional moving blood volume using quantitative three- dimensional power Doppler ultrasound. Ultrasound Med biol. 2003;29:19-23.

127. Merce lT, barco MJ, bau S. Reproducibility of the study of placental vascularization by three-dimensional power Doppler. J Perinat Med. 2004;32:228-233.

128. Merce lT, barco MJ, bau S, Kupesic S, Kurjak A. Assessment of placental vascularization by three-dimensional power Doppler "vascular biopsy" in normal

pregnancies. Croat Med J. 2005;46:765-771.

129. Hadlock FP, harrist Rb, Sharman RS et al. estimation of fetal weight with the use of head, body, and femur measurements A prospective study. AJOG. 1985;151(3):333-37.

130. Baschat AA, harman CR. Antenatal assessment of the growth restricted fetus. Curr Opin Obstet Gynecol. 2001;13:161-168.

131. Gosling RG, Dunbar G, King Dh et al. The quantitative analysis of occlusive peripheral arterial disease by a non intrusive ultrasound technique. Angiology. 1971;22:52-55.

132. Hernandez-Andrade e, brodszki J, lingman G et al. Uterine artery score and perinatal outcome. Ultrasound Obstet Gynecol. 2002 May;19(5):438-42.

133. Mari G, Deter Rl. Middle cerebral artery flow velocity waveforms in normal and small-for-gestational-age fetuses. Am J Obstet Gynecol. 1992;166:1262-1270.

134. Hofstaetter C, Dubiel M, Gudmundsson S, Maršál K. Uterine artery color Doppler assisted velocimetry and perinatal outcome. Acta Obstet Gynecol Scand. 1996;75:612-619.

135. Fuster JM. Frontal lobe and cognitive development. J neuro cytol. 2002;31:373-385.

Scientific Publications

Preliminary data of the topic of this thesis were pubblished in the following scientific Journals:

1. A. Rossi, L Forzano, G Fachechi, A Balsamo, A Adorati Menegato, I Romanello, – A new proposal of sonobiopsy of fetal brain using 3D power Doppler angiography (VOCAL) in normal and growth restricted fetuses – Ultrasound Obstet Gynecol, 36, OP 39.03 - Oct 2010.

2. A Rossi, L Forzano, G. Fachechi, A. Balsamo, A. Citossi, I. Romanello, D. Marchesoni. - Sonobiopsia fetale cerebrale mediante angiografia tridimensionale power Doppler in feti normali e IUGR: una nuova proposta – Official Proceedings Congresso Nazionale Società Italiana Ecografia Ostetrico Gincologica (SIEOG) – Sorrento. Ottobre 2010 - SIEOG News, Vol. X – Anno 2011 – Numero 2, ISSN 1594-1361.

3. A. Rossi, L. Forzano, I. Romanello – Three Dimensional cerebroplacental ratio (CPR 3DPDA): a proposal of a new parameter for the antenatal surveillance in IUGR fetuses. Ultrasound Obstet Gynecol, 38, 0P 36.08 - Oct 2011.

4. A. Rossi, L. Forzano, I. Romanello - Evaluation of fetal cerebral blood flow perfusion using power Doppler ultrasound angiography (3D-PDA) in normal and growth-restricted fetuses (IUGR). Ultrasound Obstet Gynecol, 38, OP 36.10 - Oct 2011.

5. A. Rossi, I. Romanello, L. Forzano – Evaluation of fetal cerebral blood flow perfusion using power Doppler ultrasound angiography (3D-PDA) in growth-restricted fetuses – F. V & V. in Ob Gyn. 2011, 3 (3): 175-180.

6. A. Rossi, I. Romanello, L. Forzano, G. Baccarini - Three Dimensional cerebroplacental ratio (CPR 3DPDA): a proposal of a new parameter for the antenatal surveillance in IUGR fetuses. Official Proceedings, "Advances in Fetal Imaging – US meets MRI in the Louvre" Paris – 28-29 Oct, 2011.

7. A. Rossi, L. Forzano, I. Romanello, G. Fachechi - Evaluation of fetal cerebral blood flow perfusion using power Doppler ultrasound angiography (3D-PDA) in normal and growth-restricted fetuses (IUGR). Official Proceedings, "Advances in Fetal Imaging – US meets MRI in the Louvre" Paris – 28-29 Oct, 2011.

8. A. Rossi, L. Forzano, I. Romanello, G. Baccarini - Three Dimensional cerebroplacental ratio (CPR 3DPDA): a proposal of a new parameter for the antenatal surveillance in IUGR fetuses. Official Proceedings, AIUM Annual Convention, March 29-April 1, Phoenix, Arizona (USA). Journal of Ultrasound in Medicine, 31 (suppl): S1-S136, 2012.

9. A. Rossi, I. Romanello, L. Forzano, G. Fachechi - Evaluation of fetal cerebral blood flow perfusion using power Doppler ultrasound angiography (3D-PDA) in normal and growth-restricted fetuses. Official Proceedings, AIUM Annual Convention, March 29-April 1, Phoenix, Arizona (USA). Journal of Ultrasound in Medicine, 31 (suppl): S1-S136, 2012.

10. A. Rossi, I. Romanello, L. Forzano, G. Fachechi - Evaluation of fetal cerebral blood flow perfusion using power Doppler ultrasound angiography (3D-PDA) in normal and growth-restricted fetuses (FGR). Official Proceedings, 37th International Symposium on Ultrasonic Imaging and Tissue Characterization (UITC), June 11-13, 2012 Arlington, Virginia (USA).

11. A. Rossi, L. Forzano, G. Baccarini, I. Romanello, D. Marchesoni – Three Dimensional cerebroplacental ratio (CPR 3DPDA): a new parameter for the antenatal surveillance in IUGR fetuses - Ultrasound Obstet Gynecol, 40, OP 33.07 – Sept 2012.

12. A. Rossi, I. Romanello, L. Forzano, D. Marchesoni – Evaluation of fetal cerebral perfusion using power Doppler ultrasound angiography (3D-PDA) in normal and growth-restricted fetuses (IUGR) - Ultrasound Obstet Gynecol, 40, OP 33.08 – Sept 2012.

13. A. Rossi, I. Romanello, L. Forzano, D. Marchesoni – Valutazione delle perfusione del cervello fetale mediante angiografia 3D power-doppler in feti normali e con restrizione di crescita intrauterina. – Official Proceedings XVIII Congresso Nazionale SIEOG – Genova, Maggio 2013.

14. A Rossi, I Romanello, L Forzano, M Cecchia, D Marchesoni – Assessment of Fetal Brain Vascularization using Three-Dimensional Power Doppler Ultrasound Angiography in Pregnancies affected by Fetal Growth Restriction - Official Proceedings 2nd International Conference on Fetal Growth - Baltimora (USA), Settembre 2013.

15. A. Rossi, I. Romanello, L. Forzano, M. Cecchia, G. Ambrosini, D. Marchesoni - "Assessment of Fetal Brain Vascularization using Three-Dimensional Power Doppler Ultrasound Angiography in Pregnancies Affected by Late-Onset Fetal Growth Restriction" - Global Journal of Medical Research, Vol.14, Issue 1, 2014.

16. A. Rossi, I. Romanello, L. Forzano, G. Filip, A. Citossi, D. Marchesoni - Assessment of Fetal Brain Vascularization using Three-Dimensional Power Doppler Ultrasound Angiography in Pregnancies Affected by Fetal Growth Restriction - Ultrasound Obstet Gynecol, 44, OC 20.02 - Sept 2014.

17. A. Rossi, I. Romanello, G. Filip, E. Vogrig, L. Forzano, D. Marchesoni– Assesment of fetal brain vascularization using three-dimensional power doppler ultrasound angiography in pregnancies affected by fetal growth restriction. Official Proceedings XXXIV Alpe Adria Meeting of Perinatal Medicine, Klagenfurt (Austria), Sept 2014.

Scientific Reports

Preliminary data of the topic of this thesis were presented at the following Scientific

Congresses:

1. 21th World Congress on Ultrasound in Obstetrics and Gynecology ISUOG - Los Angeles (USA) - 10-14 Ottobre 2011

2. "Advances in Fetal Imaging – US meets MRI in the Louvre" – Parigi - 28-29 Ottobre 2011

3. Annual Convention American Institute of Ultrasound in Medicine AIUM 2012 - Phoenix (USA) - 29 Marzo – 1 Aprile 2012

4. 37th International Symposium on Ultrasonic Imaging and Tissue Characterization - Arlington (USA) - 11-13 Giugno 2012

5. 22th World Congress on Ultrasound in Obstetrics and Gynecology ISUOG - Copenaghen (Denmark) - 10-13 Settembre 2012

6. XVIII Congresso Nazionale SIEOG - Genova – Maggio 2013

7. 2nd International Conference on Fetal Growth - Baltimora (USA) - 19-21 Settembre2013

8. World Congress on Ultrasound in Obstetrics and Gynecology, Barcellona (Spagna)14-17 Settembre 2014

9. XXXIV Alpe Adria Meeting of Perinatal Medicine, 26 – 27 Settembre 2014 Klagenfurt (Austria)

Acknowledgments

Thanks to…

Curiosity and Technology

Prof. Diego Marchesoni, Chief of the Department of Obstetrics and Gynecology, University of Udine